Volume 13
Number 31
21 August 2022
Pages 4455-4584

Polymer Chemistry

rsc.li/polymers

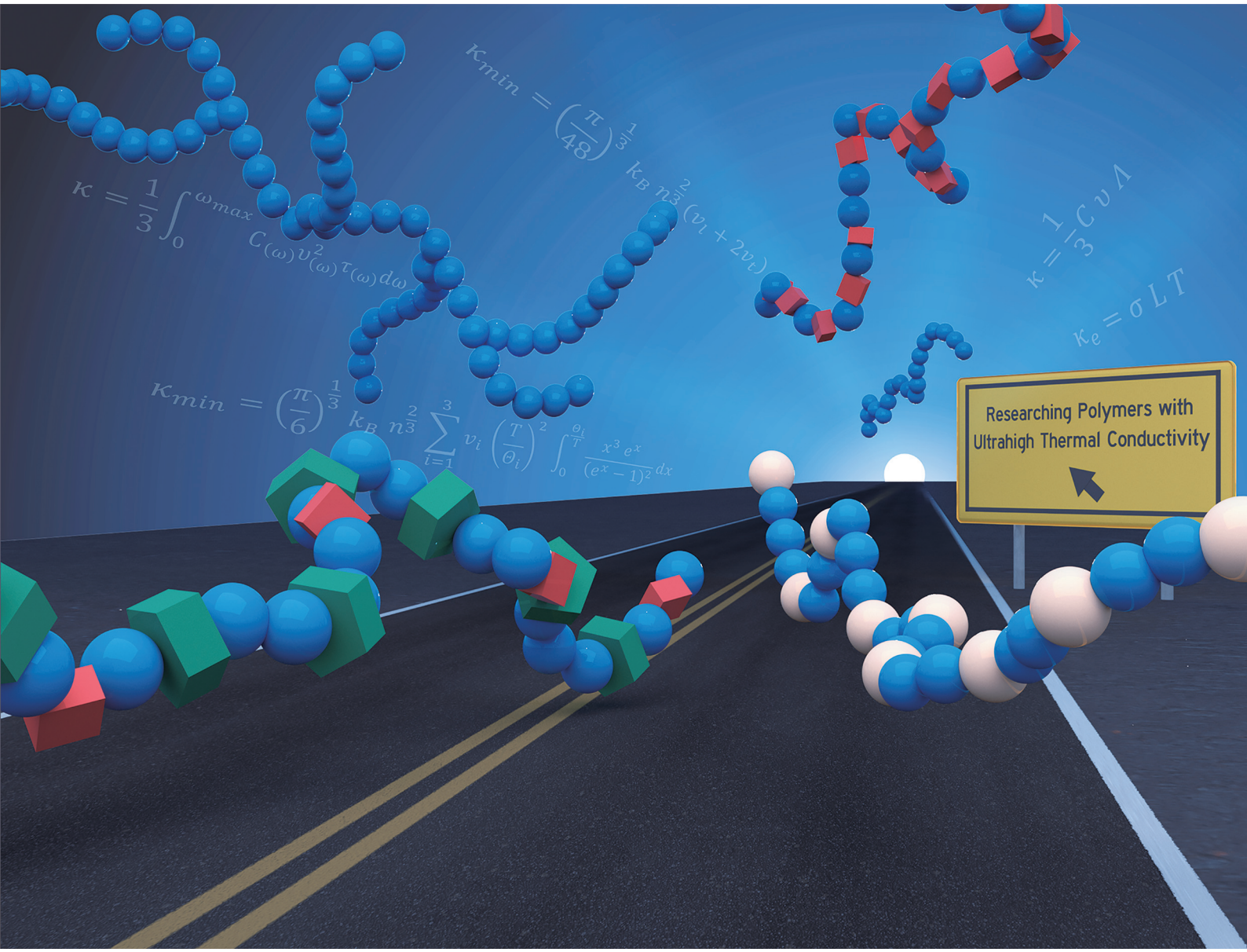

ISSN 1759-9962

ROYAL SOCIETY OF CHEMISTRY

REVIEW ARTICLE

Yanfei Xu *et al.*

State-of-the-art, opportunities, and challenges in bottom-up synthesis of polymers with high thermal conductivity

Polymer Chemistry

ROYAL SOCIETY OF CHEMISTRY

REVIEW

View Article Online
View Journal | View Issue

Check for updates

Cite this: *Polym. Chem.*, 2022, **13**, 4462

State-of-the-art, opportunities, and challenges in bottom-up synthesis of polymers with high thermal conductivity

Yurui Liu,[a] Yijie Zhou[a] and Yanfei Xu *[a,b]

In contrast to metals, polymers are predominantly thermal and electrical insulators. With their unparalleled advantages such as light weight, turning polymer insulators into heat conductors with metal-like thermal conductivity is of substantial interest and technological importance for heat dissipation applications. However, engineering bulk polymers with ultrahigh thermal conductivity remains a difficulty currently. Moreover, thermal transport mechanisms are not fully understood. In this review, we first discuss the present understanding of thermal transport mechanisms in polymers. Then, we discuss various bottom-up strategies aimed at achieving highly thermally conductive polymers with representative examples. We investigate relationships between polymer structures and thermal transport properties. We highlight current challenges within the design and synthesis of highly thermally conductive polymers. We also suggest future endeavors regarding research challenges in thermally conductive polymers. Importantly, we emphasize the potential possibilities and inspiring opportunities for future applications of thermally conductive polymers with metal-like thermal conductivity.

Received 1st March 2022,
Accepted 12th June 2022

DOI: 10.1039/d2py00272h

rsc.li/polymers

Published on 14 June 2022. Downloaded on 2/13/2026 4:19:27 PM.

Introduction

Polymers are attractive for heat dissipation applications, thanks to their unique combined properties that cannot be obtained from other materials.[1] Polymers are light weight, chemical resistant, and easily processed, to name a few.[1–3] However, common polymers are thermal insulators and have low thermal conductivities on the order of 0.1 W m^{-1} K^{-1}.[4–8] Bulk polymers have disordered chains and random defects such as chain entanglements and chain ends, which lead to low thermal conductivities in common polymers.[9–15] These thermally insulative polymers could lead to overheating problems in modern high-power-density (or high-energy-density) electronics.[16–20] To date, traditional heat conductors are metals (304-stainless steel ~15 W m^{-1} K^{-1}) and ceramics

[a]*Mechanical & Industrial Engineering Department, University of Massachusetts, Amherst, USA. E-mail: yanfeixu@umass.edu*
[b]*Chemical Engineering Department, University of Massachusetts, Amherst, USA*

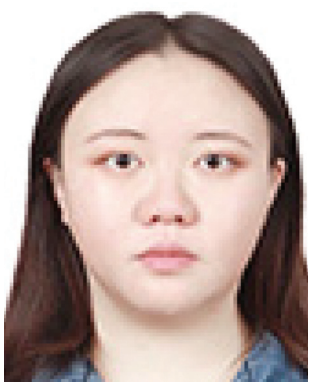

Yurui Liu

Yurui Liu is currently a Ph.D. student in the Mechanical & Industrial Engineering Department at the University of Massachusetts Amherst. Liu received her B.E. in Materials Science & Engineering at Nankai University in 2020. Her research interest is thermally conductive polymers and polymer-based composites.

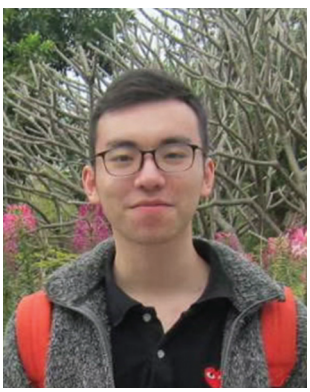

Yijie Zhou

Yijie Zhou is currently a Ph.D. student in the Mechanical & Industrial Engineering Department at the University of Massachusetts Amherst. Yijie Zhou completed his B.S. in Chemical Engineering at Central South University (China) in 2017 and received his M.S. in Chemical Engineering from South China University of Technology (China) in 2020. His current research focuses on engineered multifunctional polymers with controlled thermal conductivity.

This journal is © The Royal Society of Chemistry 2022

Published on 14 June 2022. Downloaded on 2/13/2026 4:19:27 PM.

(aluminum oxide ~30 W m^{-1} K^{-1}).[8] Thus, turning polymer insulators into heat conductors with metal-like thermal conductivity is needed.[9,21–35] Thermally conductive polymers will open up new avenues toward advanced thermal management applications such as chip packaging, soft robotics, and organic light-emitting diodes.[9,14,21,24,25,28,29,36–49]

Conventional conjugated polymers (*e.g.*, polythiophene), composed largely of conjugated carbon–carbon double bonds, possess characteristically low thermal conductivity on the order of ~0.1 W m^{-1} K^{-1}; notably, graphene is also composed of conjugated carbon–carbon double bonds.[6,8] Graphene is one of the best thermal conductors with thermal conductivity greater than ~2000 W m^{-1} K^{-1}.[50–53] This encourages research in developing thermally conductive polymers with ultrahigh thermal conductivity.[9] Atomistic simulations have also suggested that crystalline polymer chains (*e.g.*, polythiophene and polyethylene) can achieve very high—possibly divergent—thermal conductivity.[54–57] This is in agreement with the non-ergodic characteristics of one-dimensional conductors discovered by Fermi, Pasta, and Ulam (FPU).[58] However, to date, such divergent thermal conductivity suggested by simulations are not yet validated by experimental measurements.[9] Many studies try to understand the underlying physics of how, why, and under what conditions the phenomena FPU discovered will persist.[59–61] However, the synthesis of a single polymer chain is difficult.[62] The thermal conductivity measurements on a single polymer chain could also be challenging.[63]

Although there are many challenges in probing thermal transport properties in polymers, there is also exciting progress in developing the highly thermally conductive polymers.[9,10,25,28,29] For example, polyethylene,[26,29,32,64–72] thiophene-based conjugated polymers,[44,73–75] and epoxy-based polymers[13,49,76–81] with increased thermal conductivities have been developed. Details in Tables 1 and 2 will be discussed below. A high thermal conductivity of ~4.4 W m^{-1} K^{-1} in pure polythiophene nanofibers has been meassured.[75] The thermal conductivity of ultradrawn polyethylene nanofibers has been found to be as high as ~104 W m^{-1} K^{-1}, which is larger than thermal conductivities of many metals;[29] however, another challenge is finding ways to achieve scalable synthesis of bulk polymers with ultrahigh thermal conductivity larger than 100 W m^{-1} K^{-1}.[9,10] Thermal transport mechanisms in polymers have been theoretically studied, but they are not fully understood. Robust theoretical guidance for synthesizing polymers with ultrahigh thermal conductivity is lacking.[9,82] More efforts are needed to further understand the thermal transport mechanisms and explore strategies for synthesizing bulk polymers with high thermal conductivity.

The atomic-level design and synthesis of thermally conductive polymers by bottom-up approaches will provide new opportunities for making polymers with metal-like thermal conductivity, probing relationships between thermal transport properties and structures, and developing theory for better understanding thermal transport mechanisms.[34,44,75] Thermal transport properties in polymers can be manipulated through tuning the monomer composition,[4,9,10,31,83–85] crystallinity,[9,10,37,86,87] molecular weight,[88–93] type of cross-link,[88,94–100] monomer sequence of the copolymer,[101,102] intra-chain and interchain interactions,[13,33,48,97,103–112] chain orientation and assembly,[12,15,21,32,36,40,65,69,75,113–124] functional group,[12,34,82] density,[125] and/or chain morphology.[12,15,24,32,35,75,77,95,126–137] In contrast to bottom-up synthesis strategies, top-down methods, such as stretching,[29] solution shearing,[42] extrusion,[5] and thermal annealing[138] also provide new possibilities for engineering polymer chain structures and making polymers with high thermal conductivity.[4,9,28] In this review and perspective, we first discuss the current understanding of thermal transport mechanisms in crystalline solids and amorphous polymers at multiple levels ranging from the atomic level to nanoscale level. We will then highlight the strategies, progress, and challenges in designing and synthesizing highly thermally conductive polymers by bottom-up approaches at the atomic level. We also discuss the characterization techniques for measuring the thermal conductivity of bulk polymers and nanoscale polymers. We propose future research directions related to thermal transport mechanisms in polymers. Future applications of thermally conductive polymers are also highlighted. Future endeavors regarding research challenges in thermally conductive polymers are needed.

Yanfei Xu

Yanfei Xu is currently an assistant professor in the Mechanical & Industrial Engineering Department at the University of Massachusetts Amherst. She is also an adjunct assistant professor in the Chemical Engineering Department. Before joining UMASS, from 2013 to 2018, she was a postdoctoral researcher in the Mechanical Engineering Department at Massachusetts Institute of Technology, where she was active in the pursuit of turning polymer insulators into heat conductors. She also worked as a Marie Curie Fellow for the European FP7 GENIUS project at BASF & Max Planck Institute for Polymer Research Joint Lab in Germany. She received Ph.D. in Chemistry from Nankai University in 2010.

Thermal transport mechanisms in solids

Thermal conductivity characterizes materials' heat-conducting ability, which spans five orders of magnitude (~0.01–1000 W m^{-1} K^{-1}).[7,8] Diamond and graphene are among the best heat conductors and have a thermal conductivity of ~2000 W m^{-1} K^{-1} at room temperature.[7,8,11]

Published on 14 June 2022. Downloaded on 2/13/2026 4:19:27 PM.

Table 1 Intermolecular interactions promote heat conduction in polymers. Selected polymers with strong noncovalent bonds (hydrogen bonds) and high thermal conductivities (κ) include a poly(*N*-acryloyl piperidine):poly(acrylic acid) blend (PAP:PAA),[48] poly(acrylic acid) (PAA),[33] polyacrylamide (PAM),[33] poly(4-styrenesulfonic acid) (PSS),[33] polyurea,[35] poly(ethylene glycol):poly(vinyl alcohol) (PEG:PVA),[178] PVA,[179] polydehydroalanine (PDha),[34] poly(2-(imidazole-1-yl)acrylic acid) (PImAA),[34] and poly(2-(3-methylimidazolium-1-yl)acrylic acid) (PMeImAA).[34] Selected polymers with high thermal conductivities due to strong noncovalent bonds ($\pi-\pi$ interactions) between polymer chains include poly(3-hexylthiophene-2,5-diyl) (P3HT),[44] co-polyester,[109] and liquid crystal epoxies (LCEs)[13,180]

Intermolecular interactions	Polymers	Chemical structures	κ (W m^{-1} K^{-1})	Samples	Methods	Ref.
Hydrogen bonds	PAP:PAA	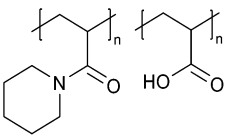	1.7 ± 0.5	Film	Spin-coating	48
	PAA		0.37 ± 0.02	Film	Spin-coating	33
	PAM	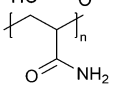	0.38 ± 0.02	Film	Spin-coating	33
	PSS	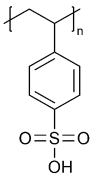	0.38 ± 0.02	Film	Spin-coating	33
	Polyurea	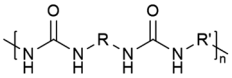	0.52 ± 0.01	Film	Casting	35
	PEG:PVA	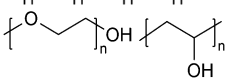	0.416	Film	Casting	178
	PVA		0.56 + 0.03	Film	Casting	179
	PDha	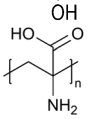	0.24 ± 0.008	Film	Spin-coating	34
	PImAA	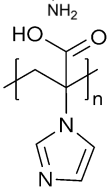	0.307 ± 0.03	Film	Spin-coating	34
	PMeImAA	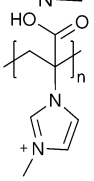	0.31 ± 0.005	Film	Spin-coating	34
$\pi-\pi$ interactions	P3HT	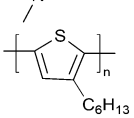	2.2 ± 0.67	Film	Oxidative Chemical Vapor Deposition (oCVD)	44
	Co-polyester	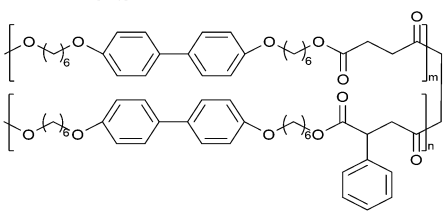	0.381	Film	Curing reaction	109

This journal is © The Royal Society of Chemistry 2022

Table 1 *(Contd.)*

Intermolecular interactions	Polymers	Chemical structures	κ (W m^{-1} K^{-1})	Samples	Methods	Ref.
	LCEs	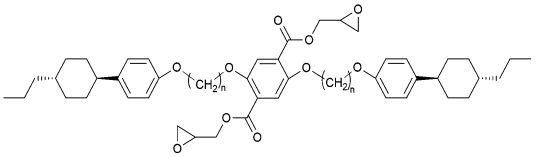	0.4	Disk	Curing reaction	13
	LCEs	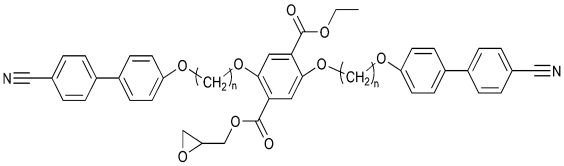	0.46	Disk	Curing reaction	180

Published on 14 June 2022. Downloaded on 2/13/2026 4:19:27 PM.

Heat in solids is mostly conducted by electrons or atomic vibrations.[7] Electrons are the main heat carriers in metals.[7,139] The electron contribution to thermal conductivity is directly related to electrical conductivity *via* the Wiedemann–Franz law (eqn (1)).[7]

$$\kappa_e = \sigma L T \tag{1}$$

where σ is electrical conductivity, L is the Lorentz number, and T is temperature.[7] Phonons are the main heat carriers in dielectric solid crystals. Phonons are quantized modes of lattice vibrations. Thermal conductivity in dielectric solid crystals is generally written as an integration over the phonon spectrum (eqn (2)).

$$\kappa = \frac{1}{3}\int_0^{\omega_{max}} C_{(\omega)} v_{(\omega)}^2 \tau_{(\omega)} \mathrm{d}\omega \tag{2}$$

where $\tau_{(\omega)}$ is the relaxation time, $v_{(\omega)}$ is the velocity of heat carriers, $C_{(\omega)}$ is the volumetric specific heat at frequency ω and temperature T, and ω is the phonon frequency. The relaxation time of the longitudinal phonons is critical to efficient heat transport.[7,32,140] The mean free path ($\Lambda_{(\omega)}$) of heat carriers is calculated using eqn (3).

$$\Lambda_{(\omega)} = v_{(\omega)} \tau_{(\omega)} \tag{3}$$

Peierls described phonon transport in dielectric materials as motion and scattering of gas particles using the Boltzmann transport equation.[141] Such a kinetic phonon gas model has laid the foundation for understanding heat conduction in semiconductor and insulator crystals (Fig. 1). Eqn (2) simply converts to eqn (4) when $\tau_{(\omega)}$ and $v_{(\omega)}$ are isotropic and are independent of frequency.

$$\kappa = \frac{1}{3} C v \Lambda \tag{4}$$

where C is the volumetric specific heat of heat carriers, v is the velocity of heat carriers, and Λ is the mean free path. In polymer single crystals, phonons can be scattered at polymer chain ends, which are boundary scattering.[9,25,92,140,142,143] Higher thermal conductivity is observed in polyethylene chains with fewer chain ends.[92] In addition to chain ends, there can also be other heat carrier scattering events such as phonon–phonon scattering.[7,9,25]

In reality, bulk polymer single crystals are rare.[62] Phonons are ill-defined in common polymers due to the lack of periodicity.[149,150] The presence of chain entanglements, voids, impurities, and other defects in common polymers leads to significant heat carrier scattering that hinders heat conduction.[14,151] Vibrational modes in amorphous solids have been classified into propagating and non-propagating modes. Allen and Feldman have introduced the terminology of "locons, diffusons, and propagons" to classify vibrational modes of disordered solids and their contributions to thermal transport.[152,153] The propagating modes are like phonons.[150,153] Diffusons exhibit a diffusive-like nature, where the vibrations are neither localized nor propagating.[144,153] Locons are localized vibrations. Fig. 1 shows fundamental differences between phonon and diffuson models of thermal transport.[144,152–157] In diffusive thermal transport mechanisms, heat is quantified by diffusons and is characterized by the diffusivity. Diffuson-based models described thermal diffusivity with random walk considerations, which leads to the jump attempt frequency ($2\omega/2\pi$) and the probability of a successful jump (P) being the operative theoretical inputs (Fig. 1).

In the random walk diffuson picture, the thermal conductivity may be estimated using eqn (5). The thermal conductivity of glass has been investigtated both theoretically and experimentally.[158,159]

$$\kappa_{diff} = \frac{1}{3} C_{(\omega)} a^2 \frac{\omega}{\pi} P \tag{5}$$

where κ_{diff} is diffusive thermal conductivity, $C_{(\omega)}$ is the volumetric specific heat, a is an interatomic distance, ω is the frequency, and P is the probability of a successful jump. In the phonon-gas model, this will correspond to $a \approx \Lambda$, which is too small to justify the use of the phonon-gas model.[153]

Cahill and Pohl have developed a minimum thermal conductivity model for predicting thermal conductivity in amorphous solids (eqn (6)).[19,33,142,148,160] This model is based on the Debye model of vibrations and assumes the lifetime of each oscillator to be half its period of vibration.[148] The

Published on 14 June 2022. Downloaded on 2/13/2026 4:19:27 PM.

Table 2 Selected thermally conductive polymers developed by various bottom-up strategies including poly(3-hexylthiophene-2,5-diyl) (P3HT),[44] poly(3,4-ethylenedioxythiophene) (PEDOT),[193] poly(3,4-ethylenedioxythiophene):Tosylate (PEDOT:Tos),[194] polythiophene (PT),[75] poly(4,8-bis-alkyloxybenzo[1,2-*b*:4,5-*b*']dithiophene-2,6-diyl-*alt*-(alkylthieno [3,4-*b*]thiophene-2-carboxylate)-2,6-diyl) (PBDTTT),[185] copolymers of 3-butylthiophene and 3-butoxythiophene (PTD),[74] high-density polyethylene (HDPE),[195] epoxy based on crosslinking reactions,[13,79,95,96] and poly(3-methylthiophene) (P3MT)-(6-(4-bromophenyl)hexyl)phosphonic acid (PHPA)[121]

Bottom-up synthesis	Polymers	Chemical structures	κ (W m^{-1} K^{-1})	Ref.
oCVD	P3HT	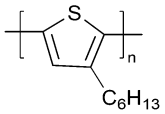	2.2 ± 0.67	44
	PEDOT	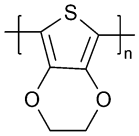	0.155 ± 0.05	193
	PEDOT:Tos	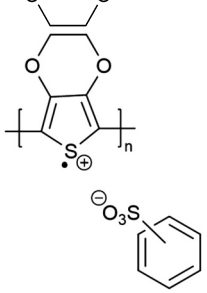	1.8 ± 0.2	194
Template-assisted method	PT	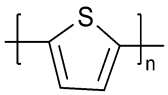	4.4 ± 0.3	75
Copoly merization	PBDTTT	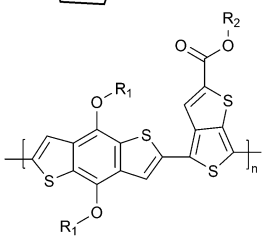	0.29 ± 0.04	185
	PTD	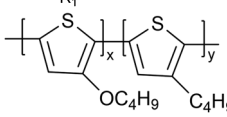	0.374	74
Crosslinking reaction	Epoxy and hardener	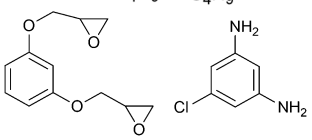	0.27 ± 0.03	95
	Epoxy and hardener	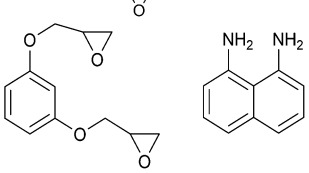	0.34 ± 0.03	96
	Epoxy and hardener	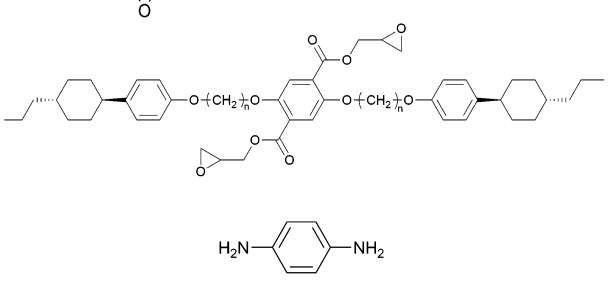	0.4	13

This journal is © The Royal Society of Chemistry 2022

Published on 14 June 2022. Downloaded on 2/13/2026 4:19:27 PM.

Table 2 *(Contd.)*

Bottom-up synthesis	Polymers	Chemical structures	κ (W m^{-1} K^{-1})	Ref.
	Epoxy and hardener	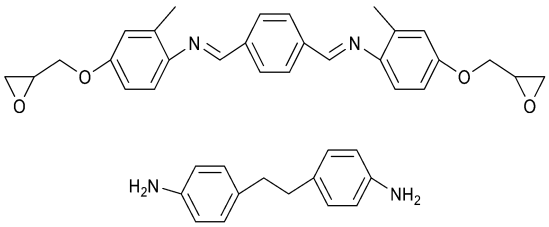	0.89	79
	HDPE	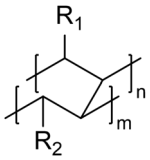	0.426	195
Surface-initiated polymerization	P3MT-PHPA	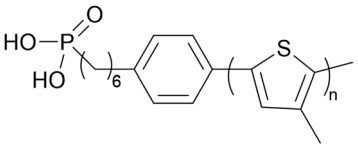	1.24 ± 0.48/0.26	121

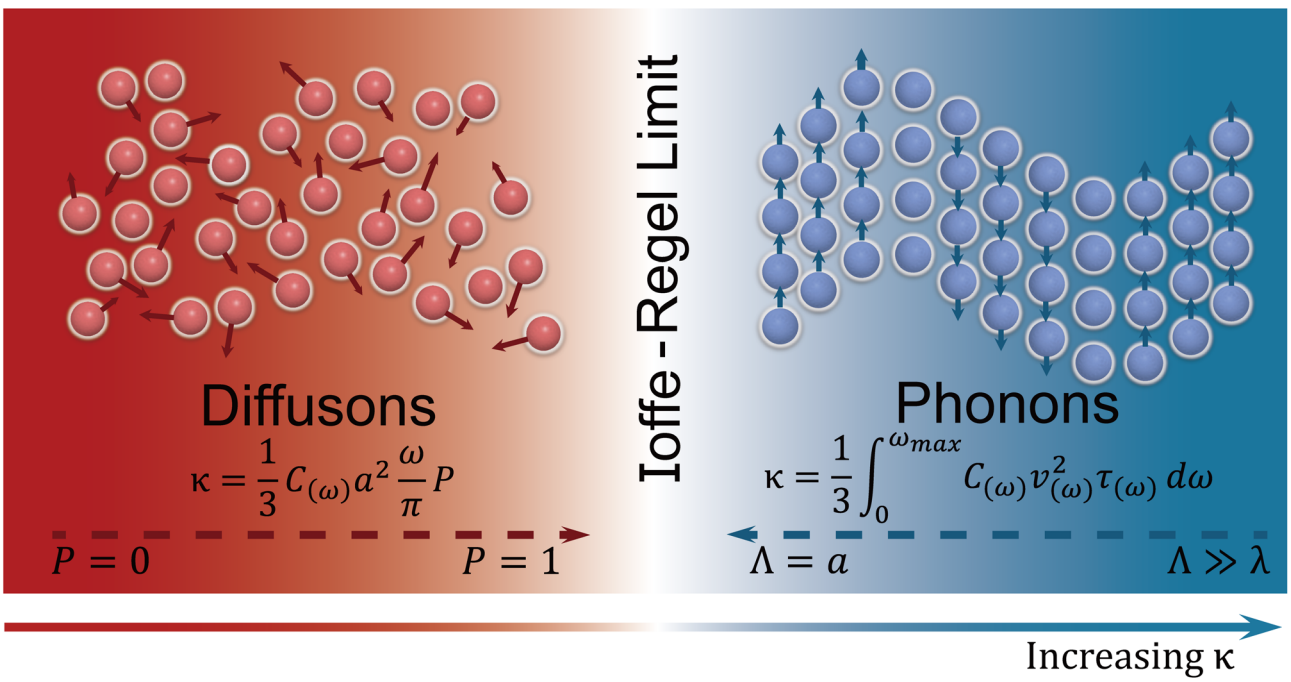

Fig. 1 Schematics of fundamental differences between diffuson and phonon models for thermal transport in solids.[144] The defining characteristics of phonon-based models include the mean free path (Λ) in thermal conductivity (κ): eqn (3) and (4). C is the volumetric specific heat, a is an interatomic distance.[145] The Ioffe–Regel limit of phonons suggest that lattice vibrations do not represent enough periodicity of the lattice to be a well-defined phonon ($\Lambda \rightarrow a$).[145] The diffuson-based model relies on thermal diffusivity coming from random walk considerations, which leads to the jump attempt frequency ($2\omega/2\pi$) and the probability of a successful jump (P) as the operative theoretical inputs in eqn (5). Slack and Cahill *et al.* have proposed a minimum thermal conductivity theory of disordered solids based on a phonon gas model, assuming that the phonon mean free paths cannot be smaller than one phonon wavelength (λ) by Slack[146,147] or half the phonon wavelength ($\lambda/2$) by Cahill.[148]

minimum thermal conductivity model was originally proposed by Einstein.[157]

$$\kappa_{\min} = \left(\frac{\pi}{6}\right)^{\frac{1}{3}} k_B n^{\frac{2}{3}} \sum_{i=1}^{3} v_i \left(\frac{T}{\Theta_i}\right)^2 \int_0^{\Theta/T} \frac{x^3 e^x}{(e^x - 1)^2} dx \quad (6)$$

where $\kappa_{\min}$ is the predicted minimum thermal conductivity, k_B is the Boltzmann constant, n is the number density of atoms, the sum is taken over the three sound modes with speeds of sound v_i (two transverse and one longitudinal), Θ_i is the cutoff temperature, $\Theta_i = v_i (\hbar/k_B) (6\pi^2 n)^{1/3}$ and $\hbar$ is the reduced

Published on 14 June 2022. Downloaded on 2/13/2026 4:19:27 PM.

Plank's constant. The models developed by Kittel,[159] Clarke,[161] Slack,[146] and Cahill[148] have shown good approximations for amorphous materials' thermal conductivities particularly at low temperatures.

In the high temperature limit, the minimum thermal conductivity has been indicated by eqn (7).[142]

$$\kappa_{min} = \left(\frac{\pi}{48}\right)^{\frac{1}{3}} k_B n^{\frac{2}{3}} (v_l + 2v_t) \quad (7)$$

where k_B is the Boltzmann constant, n is the number density of atoms, v_l is the longitudinal speed of sound, and v_t is the transverse speed of sound. Eqn (7) suggests that materials with a high number density of atoms and high sound velocity tend to possess higher thermal conductivities.[25,142] A nearly linear relationship between measured thermal conductivity and average sound velocity is shown in Fig. 2.[142] However, at room temperature, experimental thermal conductivities in fullerene derivatives have been found below the minimum thermal conductivity suggested by Cahill models.[33,162] Measured thermal conductivities in epoxy resins are found to be 10–40% lower than the predicted minimum thermal conductivity.[95] Thus, to date, thermal transport mechanisms in amorphous solids have not yet been fully understood.[25] In order to improve the predictive power for experimentalists and explain the experimental results of ultralow thermal conductivity in polymers, different models and theories are needed.

A phenomenological diffusive thermal conductivity (κ_{diff}) has recently been derived by Agne, Hanus and Snyder,[144] and it is also based on the diffusion theory of Allen and Feldman.[152–156] A diffusive thermal conductivity (κ_{diff}) could be defined as the limit of entirely diffusive thermal transport, which has been estimated using eqn (8).[144]

$$\kappa_{diff} = 0.76 k_B n^{\frac{2}{3}} \frac{1}{3} (v_l + 2v_t) \quad (8)$$

where k_B is the Boltzmann constant, n is the number density of atoms, v_l and v_t are the longitudinal speed of sound and transverse speed of sound, respectively. Compared with the minimum thermal conductivity for glass calculated with the Cahill model in eqn (6) and (7), κ_{diff} in eqn (8) could be a better estimation of a minimum thermal conductivity for materials with ultralow thermal conductivity at high temperature.[144] The relationships between thermal conductivity, the number density of atoms, and average sound velocity in eqn (6)–(8) may provide practical guides for observing the upper and/or lower limits of the thermal conductivity of amorphous solids.[107,142,144] Theoretical predictions on thermal conductivity are lacking, which causes the need for further development.[14]

Thermal conductivity gap between theory and experimental measurements of polymers

As mentioned above, polythiophene can have ultrahigh thermal conductivity along chain directions.[54,56] Atomistic simulations have suggested that an individual crystalline polythiophene chain can achieve very high—possibly divergent—thermal conductivity, in agreement with the non-ergodic characteristics of one-dimensional thermal conductors dis-

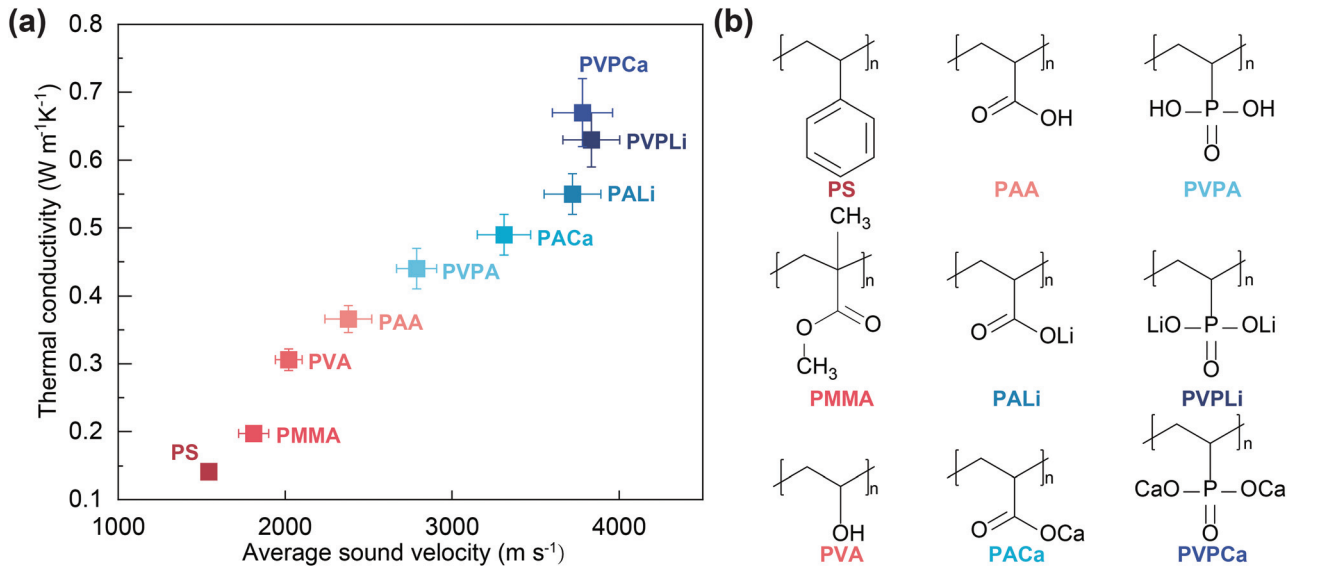

Fig. 2 (a) Relationships between measured thermal conductivities and average sound velocities of selected polymers and polymer salts, which include polystyrene (PS), polymethyl methacrylate (PMMA), polyvinyl alcohol (PVA), poly(acrylic acid) (PAA), poly(vinylphosphonic acid) (PVPA), poly (acrylic acid calcium salt) (PVPCa), poly(acrylic acid lithium salt) (PALi), poly(vinylphosphonic acid calcium salt) (PVPCa), and poly(vinylphosphonic acid lithium salt) (PVPLi).[142] These selected polymers and polymer salts have similar backbone structures with different interchain interactions. (b) Chemical structures of polymers and polymer salts.[142]

 This journal is © The Royal Society of Chemistry 2022

Published on 14 June 2022. Downloaded on 2/13/2026 4:19:27 PM.

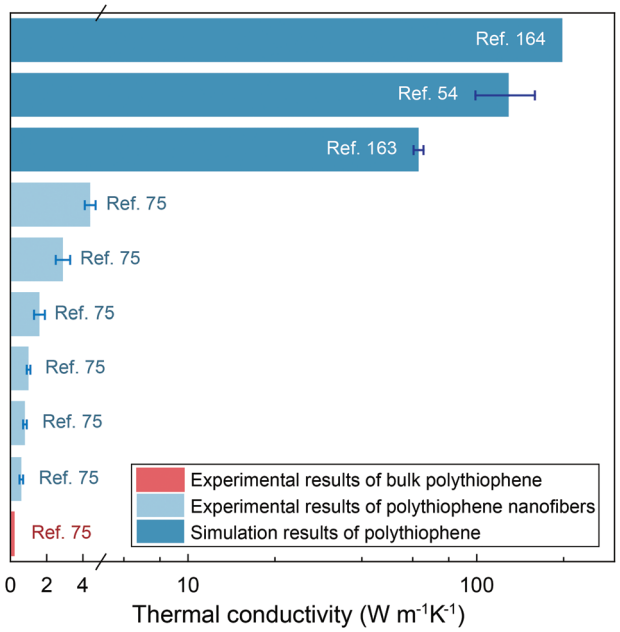

Fig. 3 Measured thermal conductivities of bulk polythiophene[75] and polythiophene nanofibers[75] at room temperature that include ~0.2 W m^{-1} K^{-1} of bulk polythiophene, ~0.6 ± 0.1 W m^{-1} K^{-1} of polythiophene nanofibers (diameter: 245 ± 5 nm), ~0.8 ± 0.1 W m^{-1} K^{-1} of polythiophene nanofibers (diameter: 204 ± 10 nm), ~0.1 ± 0.1 W m^{-1} K^{-1} of polythiophene nanofibers (diameter: 145 ± 2 nm), ~1.6 ± 0.3 W m^{-1} K^{-1} of polythiophene nanofibers (diameter: 84 ± 14 nm), ~2.9 ± 0.4 W m^{-1} K^{-1} of polythiophene nanofibers (diameter: 84 ± 12 nm), and ~4.4 ± 0.3 W m^{-1} K^{-1} of polythiophene nanofibers (diameter: 71 ± 3 nm). Simulated thermal conductivities of polythiophene that include ~62.9 ± 2.5 W m^{-1} K^{-1} of polythiophene fibers at room temperature,[163] ~129 ± 30 W m^{-1} K^{-1} along the polythiophene chain with 150 unit cells,[54] and ~198 W m^{-1} K^{-1} along the polythiophene chain axis.[164]

cussed by Fermi *et al.*[58] The thermal conductivity of bulk polythiophene is much lower than the simulated value (~198 W m^{-1} K^{-1}, Fig. 3) for polythiophene's thermal conductivity. However, the thermal conductivity of polythiophene has been enhanced through bottom-up strategies. For example, pure polythiophene nanofibers show a thermal conductivity of ~4.4 W m^{-1} K^{-1}, which is more than 20 times higher than that of bulk polythiophene.[75] This thermal conductivity enhancement results from the significant molecular chain orientation along the fiber axis that is obtained during electropolymerization using nanoscale templates, which will be discussed below.[75] Unlike drawn crystalline fibers, in these polythiophene fibers, the dominant phonon-scattering processes at room temperature is still related to structural disorders.[75] However, to date, there are no precise mechanisms that account for the discrepancy between experimental and simulated values. Efforts to synthesize thermally conductive polymers and understand thermal transport mechanisms are needed. In the section below, progress in the bottom-up synthesis of polymers with high thermal conductivity is discussed.

Common polymers have intrinsic structural disorders and random defects that act as heat carrier scattering cites.[16,27,29,165] Crystal-amorphous interfaces, chain entanglements, random coils, kinks, and chain ends in polyethylene limit macroscopic thermal properties, which result in low thermal conductivity.[26,166–169] The thermal conductivity in polymers may be crystallinity dependent. From the amorphous domains to crystalline domains, the thermal conductivity of semicrystalline polyethylene has been predicted to increase from 0.3 W m^{-1} K^{-1} to 50 W m^{-1} K^{-1} by molecular dynamics simulations.[122] However, there are exceptions. For example, polypropylene is highly crystalline but has a low thermal conductivity.[170] To achieve high thermal conductivity, methods to avoid heat carrier scattering events in polymers are needed.[171] The strength of intrachain (or interchain) interactions and conformational energy are also critical to the polymer's thermal conductivity.[9,108] High thermal conductivity has been reported in polymers with rigid backbones, for example, polyacetylene and poly-(*p*-phenylene). This is because rigid backbones can suppress segmental rotations, which can further reduce heat carrier scattering.[163,170,172] Rigid conjugated polymers such as polyacetylene[173] and poly-(*p*-phenylene)[163] could have high thermal conductivity. Conjugated ladder polymer backbones have fused rings that are π-conjugated.[174] Thus, conjugated ladder polymers may also have promising high thermal conductivities.[175] General bottom-up design strategies such as covalent annulation and noncovalent conformational control could be employed to build new rigid coplanar π systems with potential high thermal conductivities, such as thermally conductive conjugated ladder polymers.[176] Relationships between structures and thermal conductivity in these polymers need to be further investigated. Understanding these relationships could provide important principles for new polymer design and thermal management applications. Weak van der Waals forces can lead to inefficient thermal transport between polymer chains.[14,83,84,177] Thus, strong interatomic forces and intermolecular interactions may promote the exchange of thermal energy.[25,83,84] Table 1 shows the enhanced thermal conductivities observed with increasing intermolecular interactions (noncovalent bonds).

Bottom-up strategies for synthesizing polymers with high thermal conductivity

Typical strategies for enhancing efficient thermal transport in polymers are to improve chain orders (*e.g.*, chain alignments and inter-polymer chain packing),[29,56,75,106,128,163,172,181–186] to decrease interface scattering,[187–190] to increase interchain bonding (*e.g.*, hydrogen bonds and π–π interactions),[13,44,109–111,180,191] and to reduce anharmonicity/bond strength inhomogeneity.[14,146,152,192] Thus, thermally conductive polymers synthesized at monomer levels by various bottom-up approaches have been developed. The bottom-up methods include chemical vapor deposition,[44,193,194] template-assisted electrochemical polymerization,[75] copolymerization,[74,185] cross-linking reaction,[13,79,95,96,195] and surface-initiated polymerization,[121] which will be discussed below (Table 2).

Published on 14 June 2022. Downloaded on 2/13/2026 4:19:27 PM.

Chemical vapor deposition (CVD) strategies for synthesizing thermally conductive polymers

Chemical vapor deposition is a powerful technology for precisely producing high-quality polymeric conformal coatings.[196,197] Step-growth polymerization mechanisms in oxidative chemical vapor deposition (oCVD) guide the atomic-level synthesis of polymers with controllable polymer structures and well-defined chemical compositions.[198,199] As mentioned above, reducing polymer disorders and enhancing intermolecular interactions may enable efficient thermal transport in polymers. Thermally conductive conjugated poly(3-hexylthiophene) (P3HT) thin films with ordered polymer chains have been synthesized using the oCVD technique (Fig. 4).[44]

By simultaneously harnessing the strong conjugated bonds along polymer chains and the π–π interactions between them (Fig. 4d), P3HT thin films have achieved high thermal conductivities of ~2.2 W m^{-1} K^{-1} near room temperature, which is 10 times higher than that of conventional polymers.[44] Rigid polymer chains have π–π stacking structures (Fig. 4d). The 45 °C-grown P3HT film has a thermal conductivity 10 times higher than that of the 85 °C-grown P3HT film. The thermal conductivity of the 45 °C-grown P3HT increases from ~1.3 W m^{-1} K^{-1} at 200 K to ~2.2 W m^{-1} K^{-1} at 280 K and then flattens out around 300 K (Fig. 5, 45 °C-grown P3HT oCVD), which suggested the "polycrystalline" nature of the P3HT film. At low temperatures, heat carrier propagations inside the crystalline region are limited by interface scattering, and thermal conductivity increases with increasing heat carrier populations (Fig. 5, 45 °C-grown P3HT oCVD and 85 °C-grown P3HT oCVD). At higher temperatures, however, intrinsic heat carrier scattering is dominant, which could lead to decreasing thermal conductivity.[44] Poly(3,4-ethylenedioxythiophene) (PEDOT) thin films

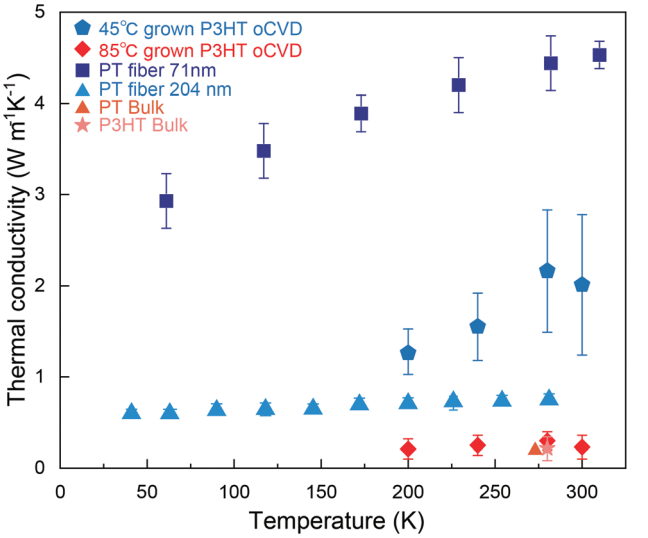

Fig. 5 Temperature-dependent thermal conductivity of poly(3-hexylthiophene-2,5-diyl) (P3HT)[201] and polythiophene (PT)[75] at near room temperature. Thermal conductivities as a function of temperatures are shown for 45 °C-grown P3HT film[44] and 85 °C-grown P3HT film[44] developed by oCVD strategies in a range from 200 to 300 K. Thermal conductivities as a function of temperatures are shown for PT fibers developed by AAO template-assisted electropolymerization with a diameter of ~71 ± 3 nm from 61 K to 310 K and PT fibers[75] with a diameter of 204 ± 10 nm from 40 K to 280 K.

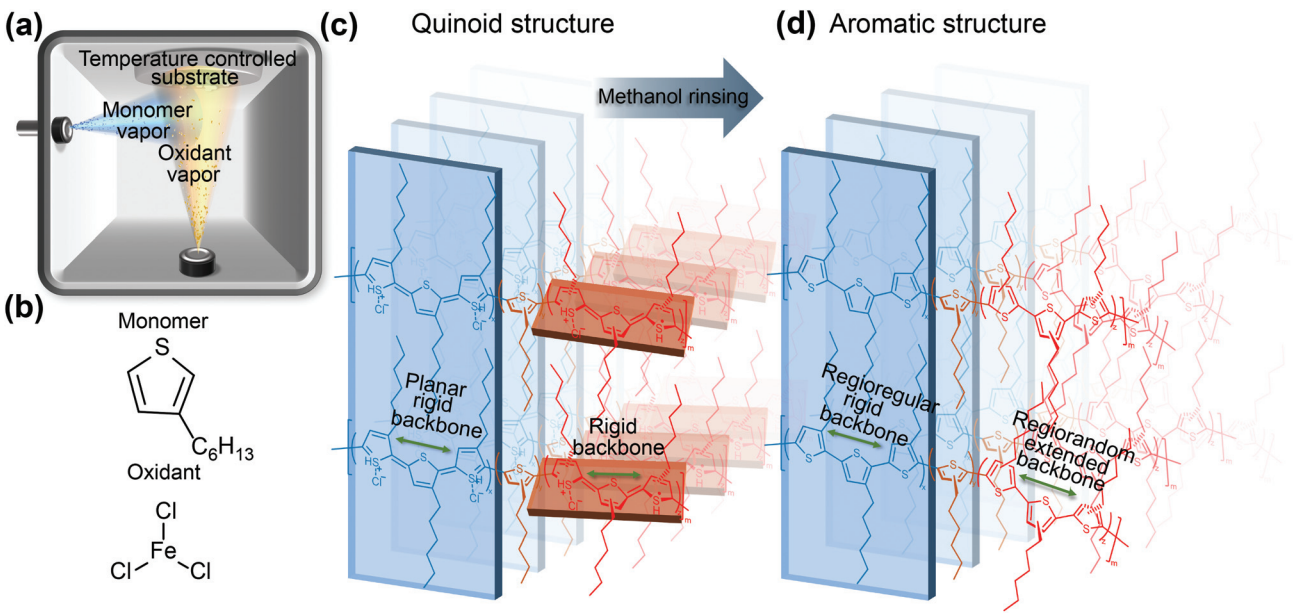

Fig. 4 (a) Schematic of an oCVD reactor for P3HT synthesis.[44] (b) Oxidants and monomers used for the synthesis of thermally conductive P3HT.[44] (c) Schematic of the microstructures of a doped P3HT film. Ordered chain grains are π–π stacking assemblies, whereas disordered chain grains have rigid backbones with suppressed distortions.[44] (d) Methanol rinsing removes excess oxidants and de-dopes (reducing) P3HT backbones. Schematic of the microstructures of the de-doped P3HT film showing ordered chain assemblies *via* π–π stacking and extended chains with suppressed distortions which originate from the quinoid structures.[44]

This journal is © The Royal Society of Chemistry 2022

Published on 14 June 2022. Downloaded on 2/13/2026 4:19:27 PM.

Table 3 Selected techniques suitable for measuring thermal conductivities of bulk, thin film, and fiber materials

	Bulk material	Thin film	Fiber
Steady-state techniques	Steady-state, absolute technique[227,229,266]	Steady-state, thermometry techniques for measuring in-plane thermal conductivities[227,229,267]	Steady-state, parallel conductance method[227,269]
	Steady-state, radial heat flow method[227,270]	Steady-state methods for measuring cross-plane thermal conductivity of thin films[227,268]	
	Steady-state, parallel conductance method[227]		
Transient techniques	Frequency-domain transient technique, pulsed power technique[227,271]	Frequency-domain transient technique, 3ω technique for measuring cross-plane thermal conductivities[272]	TDTR[32]
	Fiber aligned frequency-domain thermoreflectance technique[273]	FDTR for measuring in-plane thermal conductivities[235,274–276] and cross-plane thermal conductivities[274,276]	
	FDTR (frequency-domain thermoreflectance technique, pump probe spectroscopy)[231]	TDTR for measuring in-plane thermal conductivities[26,47,277,278] and cross-plane thermal conductivities[235]	
	TDTR (time-domain thermoreflectance technique, pump probe spectroscopy)[231]		
	Time-domain transient techniques, hot-wire method[227,279]		
	Time-domain transient techniques, laser flash method[233]		

with tailored morphologies have been synthesized using oCVD to show thermal conductivities of ~0.16 W m^{-1} K^{-1}.[193] The time-domain thermoreflectance (TDTR) technique has been used for measuring the thermal conductivity of these P3HT thin films synthesized by the oCVD technique (Table 3).[200] The differential 3ω method has been used to measure the thermal conductivity of oCVD grown PEDOT films (Table 3).[193]

Template-assisted electropolymerization strategies for synthesizing thermally conductive polymers

Electropolymerization with templates is a straightforward method to grow functional polymers at monomer levels with controlled chemical compositions, structures, and architectures (Fig. 6).[75,202–204] Anodic aluminum oxide (AAO) hard templates are widely used for electropolymerization.[205] The morphologies of polymers (*e.g.*, nanofiber diameter and length shown in Fig. 5) can be controlled by the pore diameter in AAO templates and the total charges passed through the electrochemical cell. Polythiophene nanofibers with oriented chains have been synthesized by the AAO template-assisted electropolymerization approach (Fig. 6a and b).[75] The obtained polythiophene nanofibers have controlled diameters (~71 ± 3 nm, Fig. 6c) and thermal conductivities up to ~4.4 W m^{-1} K^{-1} which is more than 20 times higher than the bulk polymer value.[75] This increased thermal conductivity of polythiophene nanofibers results from the significant molecular chain orientation along the fiber axis by AAO template-assisted electropolymerization at the nanoscale. The synthesized polymer chains in the nanofibers remain amorphous.[75]

Temperature-dependent thermal conductivities of PT fibers with different diameters (~71 ± 3 nm and 204 ± 10 nm) have been measured (Fig. 5).[75] The thermal conductivity of individual nanofibers was measured using a suspended microbridge technique.[206] The measured thermal conductivities of nanofibers increase with decreasing diameters (PT fiber: 71 nm and PT fiber: 204 nm in Fig. 5). Thermal conductivities of nanofibers with diameters of ~204 nm and ~71 nm increase monotonically from 100 K to 350 K (Fig. 5). Dominant phonon-scattering mechanisms are interchain scattering that is due to chain disorder.[75] Template-assisted electropolymerization methods may provide special opportunities for synthesizing polythiophene without side chains. Although these polythiophenes without side chains have poor solubility, they might have high thermal conductivity, because there may be less heat carrier scattering by flexible alkyl side chains. A series of poly3-alkylthiophenes with different side chain lengths have been synthesized by oxidative polymerization.[74] As the length of the side chain decreases, an increased thermal conductivity is observed and the maximum thermal conductivity reaches 0.320 W m^{-1} K^{-1} in thiophene-based polymers.[74]

In the thermal conductivity measurement experiments, Singh *et al.* have noted that the thermal conductance of nanofiber samples is low, which is on the order of 1 nW K^{-1}.[75] It is necessary to account for the background heat transfer during the thermal conductivity measurement process.[75] Neglecting this background conductance that is comparable to the sample conductance can lead to an overestimation of the thermal conductivity.[75] The background heat transfer is between the two platinum resistance thermometers *via* residual gas molecules and radiation. To eliminate the background conductance, the temperature rise on the sensing membrane was measured relative to the temperature rise on the sensing membrane of a blank device with no nanostructure. Such background elimination is carried out either with a separate background conductance measurement of a blank reference device[75,207] or simultaneously with a new differential measurement method. Details of this differential measurement are found in the references.[75,208] The background thermal conductance makes a relative

Published on 14 June 2022. Downloaded on 2/13/2026 4:19:27 PM.

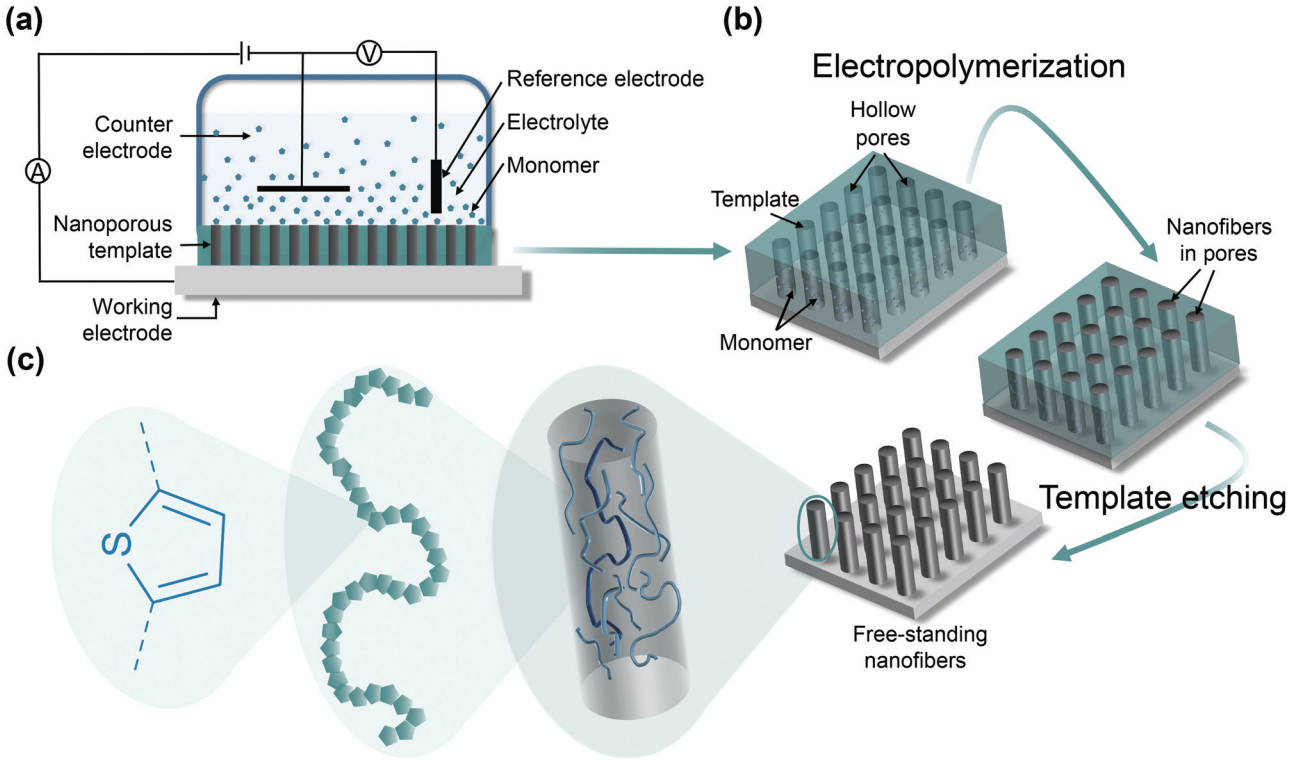

Fig. 6 (a) Schematic of the electrochemical cell for template-assisted electropolymerization with three-electrodes.[75] A metal layer (gold) coated on one side of the nanoporous anodic aluminum oxide (AAO) template is used as the working electrode.[75] Stainless steel foil is used as the counter electrode. The anodic potential is measured *versus* an Ag/AgCl reference electrode.[75] (b) Fabrication process of polymer nanofibers (*e.g.*, polythiophene nanofibers).[75] Instantaneous nucleation and subsequent two-dimensional growth occur within nanochannels of electrodes. Nanofibers are formed by electropolymerization. To dissolve the AAO template and obtain free-standing nanofiber arrays, a subsequent template etching process is introduced.[75] (c) Subsequent vertically aligned array of amorphous polymer nanofibers liberated from the AAO template with an extended conformation and improved orientation.[75] Isolated nanofiber arrays were obtained by extra neutralization and washing processes.[75] Thermal conductivities of polythiophene fibers made by AAO template-assisted electropolymerization are shown in Fig. 5.

contribution of 5% for nanofibers with diameters greater than 200 nm and between 15% and 50% for smaller nanofibers.[44,75,121]

Surface-initiated controlled polymerization strategies for growing thermally conductive polymers

The generation of polymer brushes by surface-initiated controlled radical polymerization methods has become a powerful strategy for tailoring the chemical and physical properties of interfaces. This has given rise to great advances in thermal interface materials engineering.[121,209–211] Fig. 7a shows a schematic of surface-initiated polymerization. Poly(3-methylthiophene) brushes grafted from phosphonic acid monolayers using surface-initiated polymerization have a through-plane thermal conductivity greater than ~2 W m^{-1} K^{-1}.[121] This is a 6-fold increase compared to spin-coated poly(3-hexylthiophene) samples.[121] It has been noted that the films' thicknesses are between 10 nm and 40 nm, which may be less than most application requirements. Surface-initiated controlled polymerization methods may demonstrate efficient routes toward engineering higher thermal conductivity in covalently grafted, aligned polymer films.[121]

High thermal conductivity in epoxy resins by bottom-up cross linking

New epoxy resin thermosets with tuned thermal conductivities have been designed and synthesized.[13,24,49,95,96,113,117,119,212–214] For example, to systematically investigate the relationships between thermal conductivities and molecular structures of the epoxides and hardeners, different epoxy resin thermosets from one aliphatic epoxide and one aromatic epoxide with seven amine hardeners have been developed (Fig. 8).[96] In general, aromatic structures may have higher thermal conductivities than aliphatic structures. Epoxy resin thermosets with naphthalene-based hardeners provide the highest thermal conductivity at ~0.34 W m^{-1} K^{-1} which is ~230% higher than the lowest thermal conductivity among the 14 epoxy resin thermosets (Fig. 8a).[96] The cross-linking density is controlled by mixing different molar ratios of diamine and triamine and does not influence the thermal conductivity (or longitudinal speed of sound).[96] The measured thermal conductivities of 14 epoxy resins are between ~50 and 115% of the prediction of the minimum thermal conductivity model.[96,113,212–214] Liquid crystalline epoxy resins with enhanced thermal conductivity

 This journal is © The Royal Society of Chemistry 2022

Published on 14 June 2022. Downloaded on 2/13/2026 4:19:27 PM.

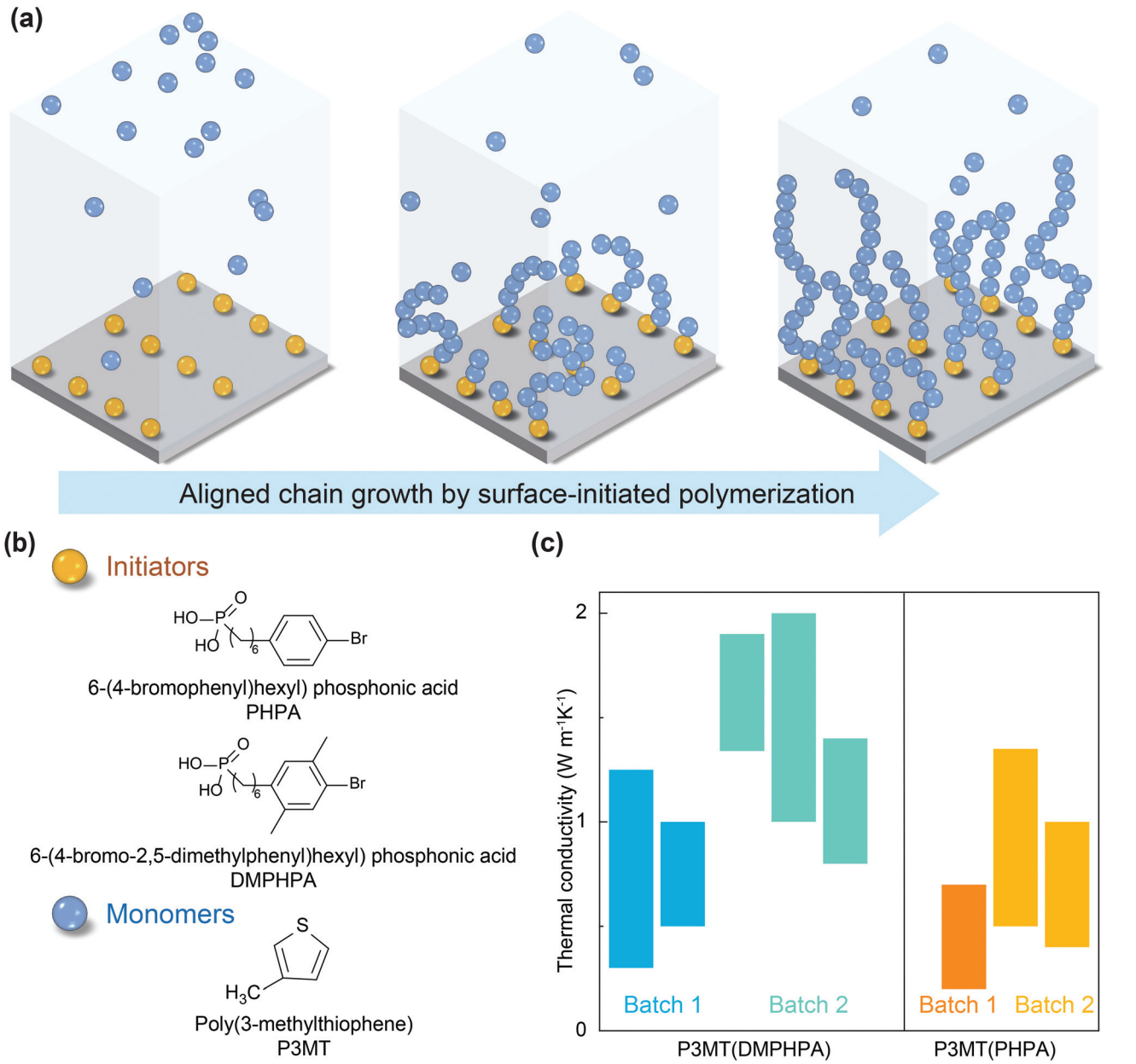

Fig. 7 (a) Schematic of surface-initiated polymerization. The substrates with a reactive initiator monolayer were immersed in monomer solution. "Polymer brushes" are grafted from the substrate through chain polymerization perpendicular to the substrate. (b) Common initiator candidates include 6-(4-bromo-2,5-dimethylphenyl)hexylphosphonic acid (DMPHPA)[121] and (6-(4-bromophenyl)hexyl)phosphonic acid (PHPA).[121] Schematic and chemical structure of a poly(3-methylthiophene) (P3MT) monomer. (c) Thermal conductivity of a poly(3-methylthiophene) (P3MT) brush initiated by 6-(4-bromo-2,5-dimethylphenyl) hexylphosphonic acid (DMPHPA) based on surface-initiated polymerization.[121] Batch 1 and batch 2 refer to P3MT samples made using the same processing at different times.[121]

have also been developed.[119] Conventional amine cross-linkers have been replaced by cationic initiators.[119] The cationic initiators are linearly woven epoxy groups tethered on microscopically aligned liquid crystal mesogens, resulting in freezing of the ordered microstructures after curing.[119] Owing to ordered structures for reducing phonon scattering during heat transport, a dramatic improvement in the thermal conductivity of neat cation-cured liquid crystalline epoxy resin has been achieved. The measured thermal conductivity is ~0.48 W m^{-1} K^{-1} which is ~141% higher than that of the amorphous amine-cured liquid crystalline epoxy resin.[119]

Ampholytic polymers with high thermal conductivity

Hydrogen bonding being ~100–1000 times greater than van der Waals interactions enables efficient thermal transport in polymers,[215] although hydrogen bonds are relatively weak compared with covalent bonds.[9,35] Thermally conductive polymers with strong hydrogen bonding have been developed

Published on 14 June 2022. Downloaded on 2/13/2026 4:19:27 PM.

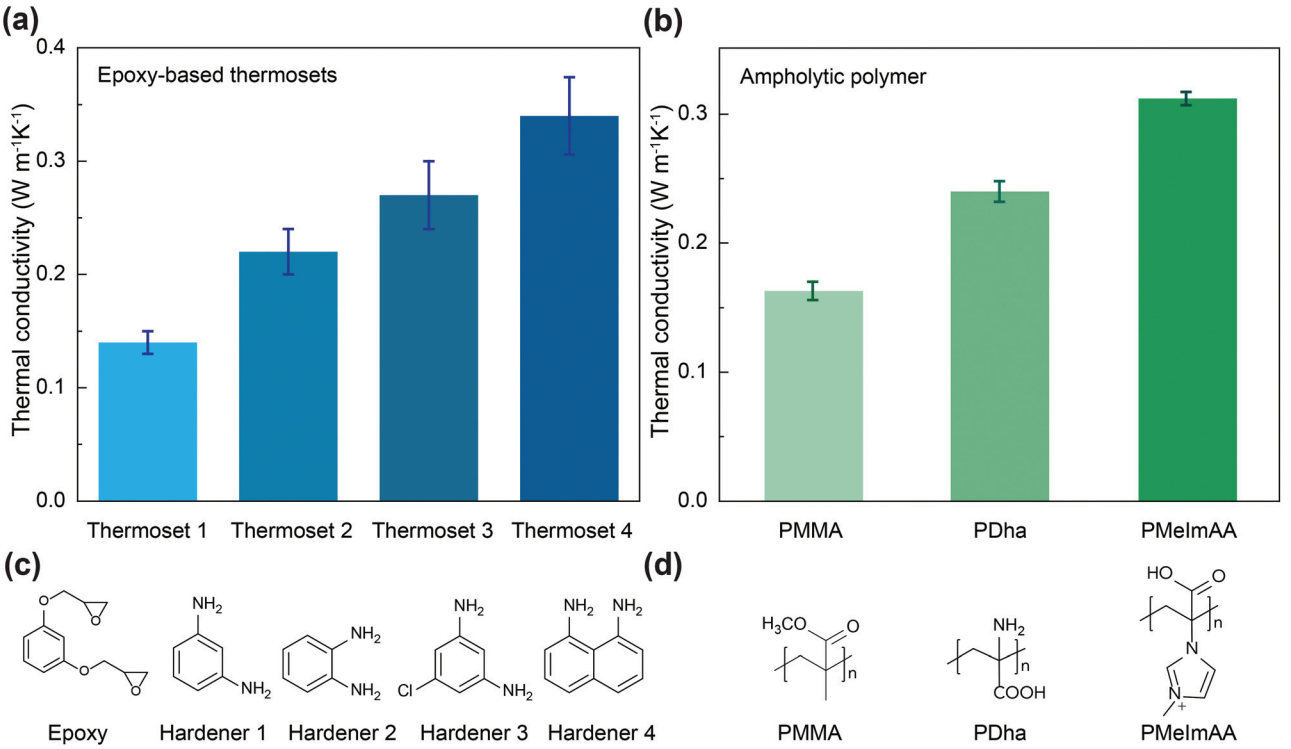

Fig. 8 (a) Thermal conductivities are shown for thermosets made by epoxy and different hardeners in (c).[95,96] (b) Thermal conductivities of ampholytic polymers including poly(methylmethacrylate),[34] (PMMA),[34] polydehydroalanine (PDha),[34] and poly(2-(3-methylimidazolium-1-yl)acrylic acid) (PMeImAA).[34] (c) Chemical structures of the selected epoxide (resorcinol diglycidyl ether) and hardeners with various functional group structures and positions. Selected hardeners include hardener 1 (*p*-phenylenediamine), hardener 2 (*o*-phenylenediamine), hardener 3 (5-chloro-*m*-phenylenediamine), and hardener 4 (1,8-diaminonaphthalene).[95,96] (d) Chemical structures of ampholytic polymers including poly(methylmethacrylate) (PMMA),[34] polydehydroalanine (PDha),[34] and poly(2-(3-methylimidazolium-1-yl)acrylic acid) (PMeImAA).[34]

(Table 1).[33–35,39,48,178,179,216,217] To investigate the relationships between thermal conductivity and interchain interactions (hydrogen bonds), several ampholytic polymers have been synthesized (Fig. 8b).[34] For the dry ampholytic polymers, Hummel *et al.* found a correlation between hydrogen bond strength and thermal conductivity.[34] Hummel *et al.* have also investigated the influence of hydration under various relative humidity conditions which mostly led to an increased thermal conductivity.[34] This increased thermal conductivity could be rationalized by the formation of a water–polymer nanocomposite material and can be described by volume-weighted mixing models.[34] Fig. 8b shows measured effective thermal conductivities of selected samples.[34]

Copolymers with high thermal conductivity

Copolymers with different segment ratios have been synthesized and their thermal transport properties have been studied (Fig. 9).[102,128] Both experimental and molecular dynamics simulation results show that the thermal conductivity of pentiptycene-based poly(*o*-hydroxyimide) increases as the ratio of the bulky pentiptycene segment increases (Fig. 9).[128] The experimental in-plane thermal conductivity is ~6 times higher than the out-of-plane value, which is due to the chain alignments in the in-plane direction.[128] The in-plane thermal conductivity at 0.982 W m^{-1} K^{-1} has been measured.[128] Experimental results show that the volumetric heat capacity increases with the bulky segment ratios which should have a positive impact on the thermal conductivity.[128] Molecular dynamics results further show that bulky segments lead to increased thermal conductivity because of polymer chain extensions and the amount of strong interatomic forces related to the aromatic carbon atoms.[128] In addition, the fractional free volume in the pentiptycene-based poly(*o*-hydroxyimide) copolymers decreases as the bulky segment ratio increases. This leads to an increase in thermal conductivity.[128]

As discussed above, high thermal conductivities have been measured in polymers, which are made by the bottom-up methods including chemical vapor deposition,[44,193,194] template-assisted electrochemical polymerization,[75] copolymerization,[74,185] cross-linking reaction,[13,79,95,96,195] and surface-initiated polymerization.[121] However, thermal transport mechanisms in these polymers are not fully understood. Molecular structural features that most influence thermal transport need to be further identified. The solid-state characterization of polymer structures will play key roles in understanding relationships between structures and thermal transport properties in polymers. For example, the synchrotron

 This journal is © The Royal Society of Chemistry 2022

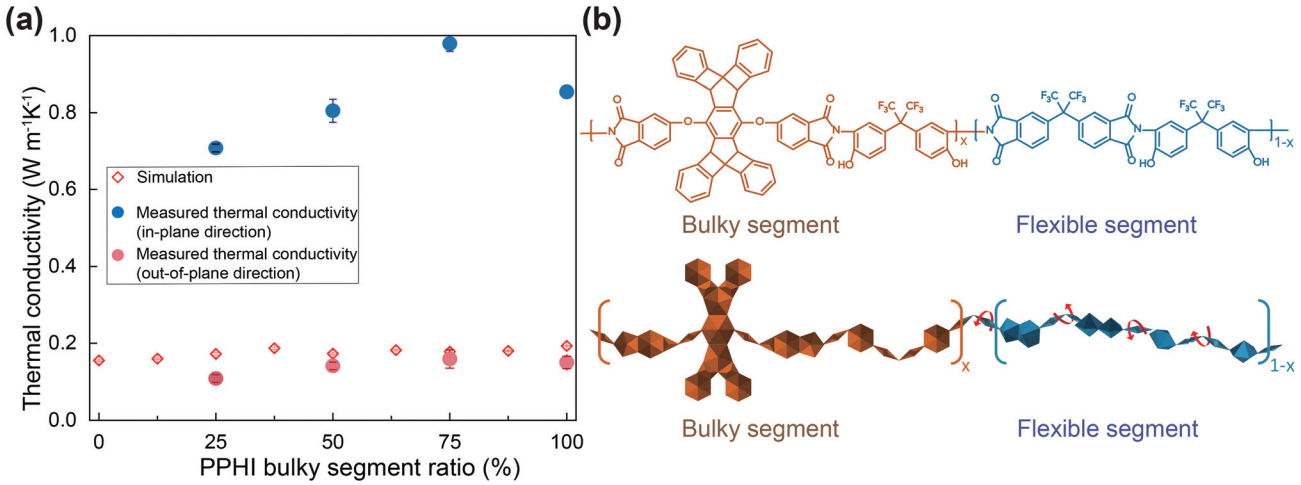

Fig. 9 (a) Relationships between the bulky segment ratio and thermal conductivity for pentiptycene-based poly(*o*-hydroxyimide) copolymers. Thermal conductivities are calculated by molecular dynamic simulation (MD simulation)[128] and experimental results for the in-plane direction and out-of-plane direction.[128] (b) Chemical structures of pentiptycene-based poly(*o*-hydroxyimide) copolymers and schematic of bulky and flexible segments.[128]

Published on 14 June 2022. Downloaded on 2/13/2026 4:19:27 PM.

wide-angle X-ray scattering (WAXS) technique is critical to determining the atomic-scale structural features of polymers, including crystallinity and crystallite orientation.[218] The small-angle X-ray scattering (SAXS) technique is essential for identifying the larger dimension features such as chain conformations.[218] The inelastic neutron scattering technique plays an important role in studying atomic vibrations and molecular motion.[218–220] Solid-state nuclear magnetic resonance (NMR) spectroscopy is important for determining molecular structures such as internuclear distances.[221–223] Raman and infrared spectroscopy play key roles in identifying vibrational modes.[224–226]

Common thermal conductivity measurement techniques

Accurate measurements of thermal conductivities of materials are important. Not only are they of fundamental scientific importance, but they are also driven by the needs of modern technology. In general, techniques applied for thermal conductivity measurements can be categorized based on the time dependence of the thermal response as steady-state methods or transient methods (Fig. 10).[227,228] The steady-state techniques measure thermal conductivity when a temperature difference between two faces of a material does not change with time.[227,229] In general, steady-state methods determine thermal conductivity directly from the proportionality between heat flow and an applied temperature difference (Fig. 10a), when a tested material's thermal state reaches complete equilibrium.[227,229] Macroscopically, the thermal conductivity of a bulk material is calculated using Fourier's law (eqn (9)).

$$q = -\kappa \nabla T \tag{9}$$

where q is the heat flux, κ is the thermal conductivity, and ∇T is the gradient of the temperature.[229]

In contrast to steady-state techniques, transient techniques usually measure the time-dependent energy dissipation process of a sample.[227,230,233–238] For example, the laser flash method is a transient technique that is one of the earliest non-contact optical techniques for measuring thermal conductivity (Fig. 10b).[233] The heat source is a short duration laser pulse. This approximates an instantaneous heat source heating one side of a sample. The thermal energy diffuses across the sample resulting in a temperature rise on the opposite side, usually measured with a thermocouple or an infrared thermometer. From the transient temperature rise, the thermal conductivity of the sample can be determined using eqn (10).

$$\kappa = \alpha \rho C_p \tag{10}$$

where κ is the thermal conductivity, α is the thermal diffusivity, ρ is density, and C_p is the mass specific heat capacity.

Laser flash techniques, which are transient techniques, have been used as ASTM standardized methods for measuring the thermal diffusivity of materials, which include polymer thin films (14–250 μm thick),[238,239] glass,[240] metals (18 μm–1 mm thick),[241–243] materials with anisotropy (*e.g.*, highly oriented thin films and graphite foil),[243] and even liquids[244,245] at both low ($T > -268$ °C)[246] and high temperatures (>1000 °C).[241]

Time-domain thermoreflectance (TDTR) is another transient, optical pump–probe technique that can measure the thermal conductivity of thin films (Fig. 10c)[230,247,248] with directionality.[32,200,249–252] The pump beam thermally excites a surface of a sample; then, the probe beam measures the time-resolved thermoreflectance of a sample.[230,236] For example, a pump beam (spot size 10–20 μm) produces an ultrashort train of pulses (~100 fs) rapidly heating the sample surface. The surface subsequently cools down after each pulse at a specific rate depending on the thermal conductivity of the sample. This surface temperature drop changes the optical reflectance

Published on 14 June 2022. Downloaded on 2/13/2026 4:19:27 PM.

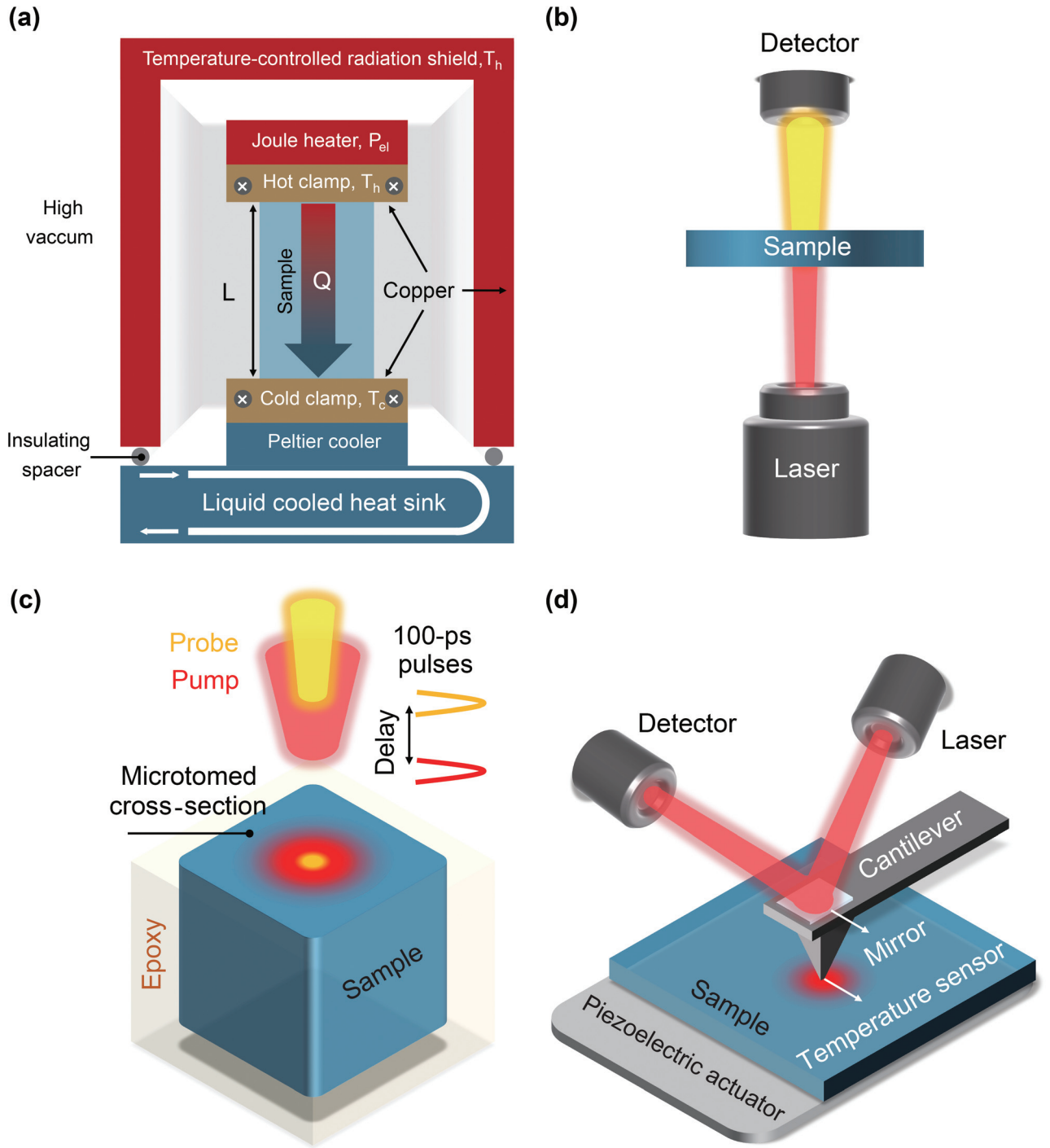

Fig. 10 (a) Schematic of a steady-state thermal conductivity measurement system.[26] A small temperature difference (T_h–T_c) across the film sample is created and maintained using Joule heating and thermoelectric cooling inside a high vacuum chamber. Please see ref. 26 for more details.[26] (b) Schematic of the laser flash method: a laser pulse heats the sample on the bottom side and a detector detects the time-dependent temperature on the top side of the sample.[230] (c) Schematic of a time-domain thermoreflectance (TDTR) system. An aluminum-coated sample could be first heated with a 100 fs-wide pump laser pulse (400 nm, red) and subsequently monitored with a time-delayed low-power probe pulse (800 nm, yellow). The change in aluminum reflectance is proportional to surface temperature variation in the linear regime.[26,231] (d) Schematic of a scanning thermal microscopy system, which uses a nanoscale heated probe to qualitatively measure the thermal conductivity of nanomaterials.[230,232]

of the sample surface (thermoreflectance). After a suitable time delay (<100 ps), the probe beam irradiates the surface and its reflection is detected by an optical sensor.[230,234] By monitoring the change in reflectance, the optical sensor measures the temperature change and ultimately the thermal conductivity using a suitable thermal transport model. A

 This journal is © The Royal Society of Chemistry 2022

Published on 14 June 2022. Downloaded on 2/13/2026 4:19:27 PM.

simple one-dimensional Cartesian heat transfer model can be used if the penetration depth is smaller than the pump beam spot size (~10–100 μm).[247,248,252,253] In the case of biomaterials, the penetration depth at ultrashort time scales (~100–1000 ps) corresponds to ~100–600 nm in biomaterials.[230]

Scanning thermal microscopy methods use a nanoscale heated probe to measure the thermal conductivity of nanoscale samples,[230,232,254–258] or temperature[259–262] on the sample surface in the range of hundreds of nanometer to micrometer range (Fig. 10d). The probe at a nanoscale of ~100 nm can be microfabricated to simultaneously function as a heater and a thermometer.[263] As shown in Fig. 10d, the probe is attached to a cantilever; the sample is on a stage. A mirror attached to a cantilever reflects light onto a photodiode to suggest the vertical and horizontal movements of the probe. As the probe scans the surface, the sample surface displaces the probe depending on its topography. The stage moves the sample to maintain a constant gap between the probe and the sample surface. During the scan, a constant current heats the probe, while the sample surface cools it, resulting in temperature decay (Fig. 10d).[232] This transient temperature change in the probe is monitored to determine the thermal conductivity of the sample near the surface.[230] To measure the thermal conductivity of an individual polyethylene fiber with diameters of 50–500 nm, Sheng Shen *et al.* have developed a general approach for thermal measurements of compliant nanofibers or nanowires using a sensitive bi-material AFM cantilever, which can resolve power measurements as low as 0.1 nW and energy measurements down to 0.15 pJ.[29,264,265]

Prospective thermal management applications of thermally conductive polymers

Thermally conductive polymers have unparalleled properties such as light weight, corrosion resistance, tunable thermal conductivity, high durability and flexibility. Thermally conductive polymers will provide new possibilities for future thermal management applications. For example, thermally conductive and electrically insulative polymers will provide new possibilities for chip packaging without overheating problems. Thermally conductive and corrosion-resistant polymer films will replace metallic heat exchangers in a wide range of applications. Thermally conductive polymers could have biological applications. Thermally conductive polymer fibers and textiles additionally will provide new opportunities for enhanced temperature control in clothing.

Conclusion

In this paper, we have discussed the state-of-the-art bottom-up strategies for synthesizing thermally conductive polymers at monomer levels. We have highlighted the basic physics of thermal transport in polymers. Both simulated and experimental results have indicated stiffer and ordered chains that may have higher thermal conductivity in the chain directions. However, the thermal conductivities of polymers are not solely controlled by bond strength. Other key structural factors play key roles in determining polymer thermal conductivities. These include crystal structures, crystallinity, monomer structures, chain conformations, and chain morphologies. To date, thermal transport mechanisms in polymers are not fully understood. A deep understanding of the relationships between thermal transport properties and structure parameters is necessary. Investigating temperature-dependent thermal conductivity in polymers is essential for a better understanding of thermal transport physics. Advancements in the fundamental understanding of thermal transport in polymers, combined with innovative bottom-up synthesis methods, will enable the production of thermally conductive polymers at large scales. We believe that thermally conductive polymers, with their unique combination of characteristics, will play key roles in many existing and unforeseen applications.

Author contributions

Yurui Liu: writing – original draft, methodology, investigation, and visualization. Yijie Zhou: investigation and visualization. Yanfei Xu: conceptualization, supervision, investigation, methodology, resources, writing – review & editing, visualization, project administration, and funding acquisition.

Conflicts of interest

There are no conflicts to declare.

Acknowledgements

The authors thank the Faculty Startup Fund Support from the University of Massachusetts Amherst. The authors thank Ms Deanna Conti, Mr Ian Goodine, and Mr Ethan Walko for proofreading the manuscript.

Notes and references

1 M. Peplow, *Nature*, 2016, **536**, 266–268.
2 A. J. Heeger, *Chem. Soc. Rev.*, 2010, **39**, 2354–2371.
3 A. J. Heeger, *Angew. Chem., Int. Ed.*, 2001, **40**, 2591–2611.
4 D. R. Anderson, *Chem. Rev.*, 1966, **66**, 677–690.
5 C. L. Choy, *Polymer*, 1977, **18**, 984–1004.
6 L. H. Sperling, *Introduction to physical polymer science*, John Wiley & Sons, Inc., 2005.
7 G. Chen, *Nanoscale Energy Transport and Conversion: A Parallel Treatment of Electrons, Molecules, Phonons, and Photons*, Oxford University Press, 2005.
8 J. H. Lienhard IV and J. H. Lienhard V, *A Heat Transfer Textbook*, Dover Publications, 5th edn, 2019.

Published on 14 June 2022. Downloaded on 2/13/2026 4:19:27 PM.

9 Y. Guo, Y. Zhou and Y. Xu, *Polymer*, 2021, **233**, 124168.
10 Y. Xu, X. Wang and Q. Hao, *Compos. Commun.*, 2021, **24**, 100617.
11 X. Qian, J. Zhou and G. Chen, *Nat. Mater.*, 2021, **20**, 1188–1202.
12 J. Lee, Y. Kim, S. R. Joshi, M. S. Kwon and G.-H. Kim, *Polym. Chem.*, 2021, **12**, 975–982.
13 Y. Kim, H. Yeo, N. H. You, S. G. Jang, S. Ahn, K. U. Jeong, S. H. Lee and M. Goh, *Polym. Chem.*, 2017, **8**, 2806–2814.
14 A. Henry, *Annu. Rev. Heat Transfer*, 2014, **17**, 485–520.
15 D. Yorifuji and S. Ando, *Macromolecules*, 2010, **43**, 7583–7593.
16 J. E. Mark, *Physical Properties of Polymers Handbook*, Springer, 2007.
17 P. Ball, *Nature*, 2012, **492**, 174–176.
18 A. L. Moore and L. Shi, *Mater. Today*, 2014, **17**, 163–174.
19 D. G. Cahill, W. K. Ford, K. E. Goodson, G. D. Mahan, A. Majumdar, H. J. Maris, R. Merlin and S. R. Phillpot, *J. Appl. Phys.*, 2002, **93**, 793–818.
20 D. G. Cahill, P. V. Braun, G. Chen, D. R. Clarke, S. Fan, K. E. Goodson, P. Keblinski, W. P. King, G. D. Mahan, A. Majumdar, H. J. Maris, S. R. Phillpot, E. Pop and L. Shi, *Appl. Phys. Rev.*, 2014, **1**, 011305.
21 H. Ko, D. G. Kang, M. Rim, J. Koo, S. I. Lim, E. Jang, D. Yu, M. J. Yoo, N. Kim and K. U. Jeong, *Polym. Chem.*, 2022, **13**, 1152–1157.
22 H. Zhang, T. Shi and A. Ma, *Polymers*, 2021, **13**, 2797.
23 W. Zhao and R. Hu, *Matter*, 2021, **4**, 3799–3801.
24 G. Lv, E. Jensen, C. M. Evans and D. G. Cahill, *ACS Appl. Polym. Mater.*, 2021, **3**, 4430–4435.
25 X. Xu, J. Zhou and J. Chen, *Adv. Funct. Mater.*, 2020, **30**, 1904704.
26 Y. Xu, D. Kraemer, B. Song, Z. Jiang, J. Zhou, J. Loomis, J. Wang, M. Li, H. Ghasemi, X. Huang, X. Li and G. Chen, *Nat. Commun.*, 2019, **10**, 1771.
27 R. Shrestha, P. Li, B. Chatterjee, T. Zheng, X. Wu, Z. Liu, T. Luo, S. Choi, K. Hippalgaonkar, M. P. de Boer and S. Shen, *Nat. Commun.*, 2018, **9**, 1664.
28 X. Xu, J. Chen, J. Zhou and B. Li, *Adv. Mater.*, 2018, **30**, 1705544.
29 S. Shen, A. Henry, J. Tong, R. Zheng and G. Chen, *Nat. Nanotechnol.*, 2010, **5**, 251–255.
30 C. T'Joen, Y. Park, Q. Wang, A. Sommers, X. Han and A. Jacobi, *Int. J. Refrig.*, 2009, **32**, 763–779.
31 M. Xiao and B. X. Du, *High Voltage*, 2016, **1**, 34–42.
32 X. Wang, V. Ho, R. A. Segalman and D. G. Cahill, *Macromolecules*, 2013, **46**, 4937–4943.
33 X. Xie, D. Li, T. H. Tsai, J. Liu, P. V. Braun and D. G. Cahill, *Macromolecules*, 2016, **49**, 972–978.
34 P. Hummel, A. M. Lechner, K. Herrmann, P. Biehl, C. Rössel, L. Wiedenhöft, F. H. Schacher and M. Retsch, *Macromolecules*, 2020, **53**, 5528–5537.
35 M. Hashimoto, H. Imoto, K. Matsukawa and K. Naka, *Macromolecules*, 2020, **53**, 2874–2881.
36 K. Ruan, Y. Guo and J. Gu, *Macromolecules*, 2021, **54**, 4934–4944.
37 H. Liu, X. Yu, M. Ji, H. Chen, G. Yang, C. Zhu and J. Xu, *Polymer*, 2021, **229**, 123975.
38 A. M. Evans, A. Giri, V. K. Sangwan, S. Xun, M. Bartnof, C. G. Torres-Castanedo, H. B. Balch, M. S. Rahn, N. P. Bradshaw, E. Vitaku, D. W. Burke, H. Li, M. J. Bedzyk, F. Wang, J. L. Brédas, J. A. Malen, A. J. H. McGaughey, M. C. Hersam, W. R. Dichtel and P. E. Hopkins, *Nat. Mater.*, 2021, **20**, 1142–1148.
39 V. P. Nguyen, D. Kim and S. M. Lee, *ACS Omega*, 2021, **6**, 29054–29059.
40 Y. Zhang, C. Lei, K. Wu and Q. Fu, *Adv. Sci.*, 2021, **8**, 2004821.
41 R. Ma, H. Zhang and T. Luo, *ACS Appl. Mater. Interfaces*, 2022, **14**, 15587–15598.
42 Z. Li, L. An, S. Khuje, J. Tan, Y. Hu, Y. Huang, D. Petit, D. Faghihi, J. Yu and S. Ren, *Sci. Adv.*, 2021, **7**, eabi7410.
43 Y. Cui, M. Li and Y. Hu, *J. Mater. Chem. C*, 2020, **8**, 10568–10586.
44 Y. Xu, X. Wang, J. Zhou, B. Song, Z. Jiang, E. M. Y. Lee, S. Huberman, K. K. Gleason and G. Chen, *Sci. Adv.*, 2018, **4**, eaar3031.
45 L. Dong, Q. Xi, D. Chen, J. Guo, T. Nakayama, Y. Li, Z. Liang, J. Zhou, X. Xu and B. Li, *Natl. Sci. Rev.*, 2018, **5**, 500–506.
46 A. R. J. Hussain, A. A. Alahyari, S. A. Eastman, C. Thibaud-Erkey, S. Johnston and M. J. Sobkowicz, *Appl. Therm. Eng.*, 2017, **113**, 1118–1127.
47 J. Liu, X. Wang, D. Li, N. E. Coates, R. A. Segalman and D. G. Cahill, *Macromolecules*, 2015, **48**, 585–591.
48 G. H. Kim, D. Lee, A. Shanker, L. Shao, M. S. Kwon, D. Gidley, J. Kim and K. P. Pipe, *Nat. Mater.*, 2015, **14**, 295–300.
49 A. I. Olamilekan and H. Yeo, *ACS Appl. Polym. Mater.*, 2021, **3**, 4147–4155.
50 A. A. Balandin, *Nat. Mater.*, 2011, **10**, 569–581.
51 J. H. Seol, I. Jo, A. L. Moore, L. Lindsay, Z. H. Aitken, M. T. Pettes, X. Li, Z. Yao, R. Huang, D. Broido, N. Mingo, R. S. Ruoff and L. Shi, *Science*, 2010, **328**, 213–216.
52 A. A. Balandin, S. Ghosh, W. Bao, I. Calizo, D. Teweldebrhan, F. Miao and C. N. Lau, *Nano Lett.*, 2008, **8**, 902–907.
53 S. Ghosh, I. Calizo, D. Teweldebrhan, E. P. Pokatilov, D. L. Nika, A. A. Balandin, W. Bao, F. Miao and C. N. Lau, *Appl. Phys. Lett.*, 2008, **92**, 151911.
54 W. Lv, R. M. Winters, F. DeAngelis, G. Weinberg and A. Henry, *J. Phys. Chem. A*, 2017, **121**, 5586–5596.
55 N. Shulumba, O. Hellman and A. J. Minnich, *Phys. Rev. Lett.*, 2017, **119**, 185901.
56 A. Henry and G. Chen, *Phys. Rev. Lett.*, 2008, **101**, 235502.
57 J. J. Freeman, G. J. Morgan and C. A. Cullen, *Phys. Rev. B: Condens. Matter Mater. Phys.*, 1987, **35**, 7627–7635.
58 E. Fermi, P. Pasta, S. Ulam and M. Tsingou, *Studies of the nonlinear problems*, University of California, 1955.
59 G. P. Berman and F. M. Izrailev, *Chaos*, 2005, **15**, 015104.
60 M. Toda, *Phys. Rep.*, 1975, **18**, 1–123.
61 R. Livi, M. Pettini, S. Ruffo, M. Sparpaglione and A. Vulpiani, *Phys. Rev. A*, 1985, **31**, 1039–1045.

 This journal is © The Royal Society of Chemistry 2022

Published on 14 June 2022. Downloaded on 2/13/2026 4:19:27 PM.

62 B. Lotz, T. Miyoshi and S. Z. D. Cheng, *Macromolecules*, 2017, **50**, 5995–6025.
63 L. Cui, S. Hur, Z. A. Akbar, J. C. Klöckner, W. Jeong, F. Pauly, S.-Y. Jang, P. Reddy and E. Meyhofer, *Nature*, 2019, **572**, 628–633.
64 Q. Zhang, L. Lan, Z. Zheng, P. Liu, H. Wu, S. Guo, C. Lin and G. He, *Polymer*, 2022, **241**, 124532.
65 A. A. Candadai, J. A. Weibel and A. M. Marconnet, *ACS Appl. Polym. Mater.*, 2020, **2**, 437–447.
66 Y. F. Huang, Z. G. Wang, W. C. Yu, Y. Ren, J. Lei, J. Z. Xu and Z. M. Li, *Polymer*, 2019, **180**, 121760.
67 R. C. Zhang, Z. Huang, D. Sun, D. Ji, M. Zhong, D. Zang, J. Z. Xu, Y. Wan and A. Lu, *Polymer*, 2018, **154**, 42–47.
68 S. Ronca, T. Igarashi, G. Forte and S. Rastogi, *Polymer*, 2017, **123**, 203–210.
69 Y. Lu, J. Liu, X. Xie and D. G. Cahill, *ACS Macro Lett.*, 2016, **5**, 646–650.
70 C. L. Choy, Y. W. Wong, G. W. Yang and T. Kanamoto, *J. Polym. Sci., Part B: Polym. Phys.*, 1999, **37**, 3359–3367.
71 D. Hansen and G. A. Bernier, *Polym. Eng. Sci.*, 1972, **12**, 204–208.
72 C. L. Choy, W. H. Luk and F. C. Chen, *Polymer*, 1978, **19**, 155–162.
73 W. Liu, Z. Lei, R. Yang, W. Xing, P. Tao, W. Shang, B. Fu, C. Song and T. Deng, *ACS Appl. Mater. Interfaces*, 2022, **14**, 10605–10615.
74 H. Zheng, K. Wu, W. Chen, B. Nan, Z. Qu and M. Lu, *Macromol. Chem. Phys.*, 2021, **222**, 2000418.
75 V. Singh, T. L. Bougher, A. Weathers, Y. Cai, K. Bi, M. T. Pettes, S. A. McMenamin, W. Lv, D. P. Resler, T. R. Gattuso, D. H. Altman, K. H. Sandhage, L. Shi, A. Henry and B. A. Cola, *Nat. Nanotechnol.*, 2014, **9**, 384–390.
76 D. G. Kang, H. Ko, J. Koo, S. I. Lim, J. S. Kim, Y. T. Yu, C. R. Lee, N. Kim and K. U. Jeong, *ACS Appl. Mater. Interfaces*, 2018, **10**, 35557–35562.
77 S. J. Ge, T. P. Zhao, M. Wang, L. L. Deng, B. P. Lin, X. Q. Zhang, Y. Sun, H. Yang and E. Q. Chen, *Soft Matter*, 2017, **13**, 5463–5468.
78 J. Shin, M. Kang, T. Tsai, C. Leal, P. V. Braun and D. G. Cahill, *ACS Macro Lett.*, 2016, **5**, 955–960.
79 M. Harada, M. Ochi, M. Tobita, T. Kimura, T. Ishigaki, N. Shimoyama and H. Aoki, *J. Polym. Sci., Part B: Polym. Phys.*, 2003, **41**, 1739–1743.
80 A. Hammerschmidt, K. Geibel and F. Strohmer, *Adv. Mater.*, 1993, **5**, 107–109.
81 K. Kanari and T. Ozawa, *Polym. J.*, 1973, **4**, 372–378.
82 K. Utimula, T. Ichibha, R. Maezono and K. Hongo, *Chem. Mater.*, 2019, **31**, 4649–4656.
83 Y. Guo, K. Ruan, X. Shi, X. Yang and J. Gu, *Compos. Sci. Technol.*, 2020, **193**, 108134.
84 C. Huang, X. Qian and R. Yang, *Mater. Sci. Eng., R*, 2018, **132**, 1–22.
85 X. Wei and T. Luo, *Phys. Chem. Chem. Phys.*, 2018, **20**, 20534–20539.
86 J. Yu, B. Sundqvist, B. Tonpheng and O. Andersson, *Polymer*, 2014, **55**, 195–200.
87 D. Greig, *Cryogenics*, 1988, **28**, 243–247.
88 J. M. Rinehart, J. R. Reynolds and S. K. Yee, *ACS Appl. Polym. Mater.*, 2022, **4**, 1218–1224.
89 Y. Du, S. Liu, S. Yuan, H. Zhang and S. Yuan, *Colloids Surf., A*, 2021, **618**, 126409.
90 A. Kiessling, D. N. Simavilla, G. G. Vogiatzis and D. C. Venerus, *Polymer*, 2021, **228**, 123881.
91 X. Pan, A. H. P. J. Schenning, L. Shen and C. W. M. Bastiaansen, *Macromolecules*, 2020, **53**, 5599–5603.
92 B. Zhang, P. Mao, Y. Liang, Y. He, W. Liu and Z. Liu, *ES Energy Environ.*, 2019, **5**, 37–55.
93 Y. Zhang, X. Zhang, L. Yang, Q. Zhang, M. L. Fitzgerald, A. Ueda, Y. Chen, R. Mu, D. Li and L. M. Bellan, *Soft Matter*, 2018, **14**, 9534–9541.
94 S. Rbihi, L. Laallam, O. Bayousfi, A. Moubarik, A. Liba and A. Jouaiti, *J. Therm. Anal. Calorim.*, 2022, DOI: **10.1007/s10973-021-11189-0**.
95 G. Lv, E. Jensen, C. Shen, K. Yang, C. M. Evans and D. G. Cahill, *ACS Appl. Polym. Mater.*, 2021, **3**, 259–267.
96 G. Lv, E. Jensen, N. Shan, C. M. Evans and D. G. Cahill, *ACS Appl. Polym. Mater.*, 2021, **3**, 1555–1562.
97 G. Lv, B. Soman, N. Shan, C. M. Evans and D. G. Cahill, *ACS Macro Lett.*, 2021, **10**, 1088–1093.
98 S. Li, X. Yu, H. Bao and N. Yang, *J. Phys. Chem. C*, 2018, **122**, 13140–13147.
99 O. Yamamoto, *Polym. J.*, 1971, **2**, 509–517.
100 O. Yamamoto and H. Kambe, *Polym. J.*, 1971, **2**, 623–628.
101 T. Zhou, Z. Wu, H. K. Chilukoti and F. Müller-Plathe, *J. Chem. Theory Comput.*, 2021, **17**, 3772–3782.
102 R. Li, J. A. Ton Loontjens and Z. Shan, *Eur. Polym. J.*, 2019, **112**, 423–432.
103 X. Ran, Y. Wang, J. Lu, R. Sun, J. B. Xu, N. Yang, H. Yin and C. P. Wong, *Comput. Mater. Sci.*, 2022, **205**, 111191.
104 T. Meng, Y. Sun, C. Tong, P. Zhang, D. Xu, J. Yang, P. Gu, J. Yang and Y. Zhao, *Nano Lett.*, 2021, **21**, 3843–3848.
105 Y. Ouyang, C. Yu, G. Yan and J. Chen, *Front. Phys.*, 2021, **16**, 43200.
106 A. Chen, Y. Wu, S. Zhou, W. Xu, W. Jiang, Y. Lv, W. Guo, K. Chi, Q. Sun, T. Fu, T. Xie, Y. Zhu and X. G. Liang, *Mater. Adv.*, 2020, **1**, 1996–2002.
107 X. Wei, R. Ma and T. Luo, *J. Phys. Chem. C*, 2020, **124**, 4483–4488.
108 M. X. Zhu, H. G. Song, Q. C. Yu, J. M. Chen and H. Y. Zhang, *Int. J. Heat Mass Transfer*, 2020, **162**, 120381.
109 W. Chen, K. Wu, Z. Qu and M. Lu, *Eur. Polym. J.*, 2019, **121**, 109275.
110 A. Shanker, C. Li, G. H. Kim, D. Gidley, K. P. Pipe and J. Kim, *Sci. Adv.*, 2017, **3**, e1700342.
111 X. Wei, T. Zhang and T. Luo, *Phys. Chem. Chem. Phys.*, 2016, **18**, 32146–32154.
112 E. Lussetti, T. Terao and F. Müller-Plathe, *J. Phys. Chem. B*, 2007, **111**, 11516–11523.

Published on 14 June 2022. Downloaded on 2/13/2026 4:19:27 PM.

113 X. Zhong, X. Yang, K. Ruan, J. Zhang, H. Zhang and J. Gu, *Macromol. Rapid Commun.*, 2022, **43**, 2100580.
114 T. Wu, J. Zhu, H. Yu, S. Qu and W. Yang, *Int. J. Heat Mass Transfer*, 2022, **185**, 122445.
115 S. Deng, J. Yuan, Y. Lin, X. Yu, D. Ma, Y. Huang, R. Ji, G. Zhang and N. Yang, *Nano Energy*, 2021, **82**, 105749.
116 A. A. Candadai, E. J. Nadler, J. S. Burke, J. A. Weibel and A. M. Marconnet, *Sci. Rep.*, 2021, **11**, 8705.
117 Q. Zhang, T. Zhang, Y. Zhou, C. Li, H. Wu and S. Guo, *Polym. J.*, 2021, **53**, 1371–1381.
118 B. F. Donovan, R. J. Warzoha, T. Cosby, A. Giri, A. A. Wilson, A. J. Borgdorff, N. T. Vu, E. A. Patterson and E. P. Gorzkowski, *Macromolecules*, 2020, **53**, 11089–11097.
119 A. M. Islam, H. Lim, N. H. You, S. Ahn, M. Goh, J. R. Hahn, H. Yeo and S. G. Jang, *ACS Macro Lett.*, 2018, **7**, 1180–1185.
120 C. Lu, S. W. Chiang, H. Du, J. Li, L. Gan, X. Zhang, X. Chu, Y. Yao, B. Li and F. Kang, *Polymer*, 2017, **115**, 52–59.
121 A. Roy, T. L. Bougher, R. Geng, Y. Ke, J. Locklin and B. A. Cola, *ACS Appl. Mater. Interfaces*, 2016, **8**, 25578–25585.
122 T. Zhang and T. Luo, *ACS Nano*, 2013, **7**, 7592–7600.
123 D. C. Venerus and D. N. Kolev, *Macromolecules*, 2009, **42**, 2594–2598.
124 M. D. Losego, L. Moh, K. A. Arpin, D. G. Cahill and P. V. Braun, *Appl. Phys. Lett.*, 2010, **97**, 011908.
125 A. Leroy, B. Bhatia, J. Sircar and E. N. Wang, *Int. J. Heat Mass Transfer*, 2022, **184**, 122307.
126 P. S. Jadhav, G. M. Joshi, S. S. Humbe, R. S. Dubey and S. Kaleemulla, *Polym. Int.*, 2022, DOI: **10.1002/pi.6385**.
127 M. Antlauf, N. Boulanger, L. Berglund, K. Oksman and O. Andersson, *Biomacromolecules*, 2021, **22**, 3800–3809.
128 X. Wei, Z. Huang, S. Koch, M. Zamengo, Y. Deng, M. L. Minus, J. Morikawa, R. Guo and T. Luo, *ACS Appl. Polym. Mater.*, 2021, **3**, 2979–2987.
129 E. Selezneva, R. D. Pietro, X. Jiao, C. R. McNeill and H. Sirringhaus, *APL Mater.*, 2019, **7**, 081118.
130 J. A. Tomko, A. Pena-Francesch, H. Jung, M. Tyagi, B. D. Allen, M. C. Demirel and P. E. Hopkins, *Nat. Nanotechnol.*, 2018, **13**, 959–964.
131 J. C. Williams, B. N. Nguyen, L. McCorkle, D. Scheiman, J. S. Griffin, S. A. Steiner and M. A. B. Meador, *ACS Appl. Mater. Interfaces*, 2017, **9**, 1801–1809.
132 B. Zhu, J. Liu, T. Wang, M. Han, S. Valloppilly, S. Xu and X. Wang, *ACS Omega*, 2017, **2**, 3931–3944.
133 J. Liu, Z. Xu, Z. Cheng, S. Xu and X. Wang, *ACS Appl. Mater. Interfaces*, 2015, **7**, 27279–27288.
134 Z. Guo, D. Lee, J. Strzalka, H. Gao, L. Huang, A. M. Khounsary and T. Luo, *Phys. Chem. Chem. Phys.*, 2014, **16**, 26359–26364.
135 W. N. dos Santos, J. A. de Sousa and R. Gregorio, *Polym. Test.*, 2013, **32**, 987–994.
136 S. Okamoto and H. Ishida, *Macromolecules*, 2001, **34**, 7392–7402.
137 Y. Kawamura, *Polym. J.*, 1970, **1**, 480–484.
138 H. Prajapati, D. Chalise, D. Ravoori, R. M. Taylor and A. Jain, *Addit. Manuf.*, 2019, **26**, 242–249.
139 Y. Quan, S. Yue and B. Liao, *Nanoscale Microscale Thermophys. Eng.*, 2021, **25**, 73–90.
140 J. Liu and R. Yang, *Phys. Rev. B: Condens. Matter Mater. Phys.*, 2012, **86**, 104307.
141 R. Peierls, *Ann. Phys.*, 1929, **395**, 1055–1101.
142 X. Xie, K. Yang, D. Li, T. H. Tsai, J. Shin, P. V. Braun and D. G. Cahill, *Phys. Rev. B*, 2017, **95**, 035406.
143 N. W. Ashcroft and N. D. Mermin, *Solid state physics*, Holt, Rinehart and Winston, New York, 1976.
144 M. T. Agne, R. Hanus and G. J. Snyder, *Energy Environ. Sci.*, 2018, **11**, 609–616.
145 A. Ioffe and A. Regel, *Prog. Semicond.*, 1960, **6**, 237–291.
146 G. A. Slack, *J. Phys. Chem. Solids*, 1973, **34**, 321–335.
147 G. A. Slack, in *Solid State Phys*, ed. H. Ehrenreich, F. Seitz and D. Turnbull, Academic Press, 1979, vol. 34, pp. 1–71.
148 D. G. Cahill, S. K. Watson and R. O. Pohl, *Phys. Rev. B: Condens. Matter Mater. Phys.*, 1992, **46**, 6131–6140.
149 Q. Xi, J. Zhong, J. He, X. Xu, T. Nakayama, Y. Wang, J. Liu, J. Zhou and B. Li, *Chin. Phys. Lett.*, 2020, **37**, 104401.
150 S. Kommandur and S. K. Yee, *J. Polym. Sci., Part B: Polym. Phys.*, 2017, **55**, 1160–1170.
151 S. Lin, Z. Cai, Y. Wang, L. Zhao and C. Zhai, *npj Comput. Mater.*, 2019, **5**, 26.
152 P. B. Allen and J. L. Feldman, *Phys. Rev. B: Condens. Matter Mater. Phys.*, 1993, **48**, 12581–12588.
153 P. B. Allen, J. L. Feldman, J. Fabian and F. Wooten, *Philos. Mag. B*, 1999, **79**, 1715–1731.
154 J. L. Feldman, P. B. Allen and S. R. Bickham, *Phys. Rev. B: Condens. Matter Mater. Phys.*, 1999, **59**, 3551–3559.
155 J. L. Feldman, M. D. Kluge, P. B. Allen and F. Wooten, *Phys. Rev. B: Condens. Matter Mater. Phys.*, 1993, **48**, 12589–12602.
156 P. B. Allen and J. L. Feldman, *Phys. Rev. Lett.*, 1989, **62**, 645–648.
157 A. Einstein, *Ann. Phys.*, 1911, **340**, 679–694.
158 A. F. Birch and H. Clark, *Am. J. Sci.*, 1940, **238**, 529–558.
159 C. Kittel, *Phys. Rev.*, 1949, **75**, 972–974.
160 D. G. Cahill and R. O. Pohl, *Phys. Rev. B: Condens. Matter Mater. Phys.*, 1987, **35**, 4067–4073.
161 D. R. Clarke, *Surf. Coat. Technol.*, 2003, **163–164**, 67–74.
162 L. Chen, X. Wang and S. Kumar, *Sci. Rep.*, 2015, **5**, 12763.
163 T. Zhang, X. Wu and T. Luo, *J. Phys. Chem. C*, 2014, **118**, 21148–21159.
164 P. Cheng, N. Shulumba and A. J. Minnich, *Phys. Rev. B*, 2019, **100**, 094306.
165 P. Dashora and G. Gupta, *Polymer*, 1996, **37**, 231–234.
166 M. Schulz, M. Schäfer, K. Saalwächter and T. Thurn-Albrecht, *Nat. Commun.*, 2022, **13**, 119.
167 S. Datta, S. Takahashi and S. Yagai, *Acc. Mater. Res.*, 2022, **3**, 259–271.
168 X. Duan, Z. Li, J. Liu, G. Chen and X. Li, *J. Appl. Phys.*, 2019, **125**, 164303.

 This journal is © The Royal Society of Chemistry 2022

Published on 14 June 2022. Downloaded on 2/13/2026 4:19:27 PM.

169 R. C. Savage, N. Mullin and J. K. Hobbs, *Macromolecules*, 2015, **48**, 6160–6165.
170 H. Chen, V. V. Ginzburg, J. Yang, Y. Yang, W. Liu, Y. Huang, L. Du and B. Chen, *Prog. Polym. Sci.*, 2016, **59**, 41–85.
171 H. R. Seyf, L. Yates, T. L. Bougher, S. Graham, B. A. Cola, T. Detchprohm, M. H. Ji, J. Kim, R. Dupuis, W. Lv and A. Henry, *npj Comput. Mater.*, 2017, **3**, 49.
172 T. Zhang and T. Luo, *J. Phys. Chem. B*, 2016, **120**, 803–812.
173 L. Piraux, M. Kinany-Alaoui, J. P. Issi, D. Begin and D. Billaud, *Solid State Commun.*, 1989, **70**, 427–429.
174 T. M. Swager, *Macromolecules*, 2017, **50**, 4867–4886.
175 J. Lee, A. J. Kalin, T. Yuan, M. Al-Hashimi and L. Fang, *Chem. Sci.*, 2017, **8**, 2503–2521.
176 C. Zhu, A. J. Kalin and L. Fang, *Acc. Chem. Res.*, 2019, **52**, 1089–1100.
177 T. Luo and G. Chen, *Phys. Chem. Chem. Phys.*, 2013, **15**, 3389–3412.
178 N. Mehra, L. Mu and J. Zhu, *Compos. Sci. Technol.*, 2017, **148**, 97–105.
179 J. Zhou, S. Lin, H. Zeng, J. Liu, B. Li, Y. Xu, X. Zhao and G. Chen, *Mater. Horiz.*, 2020, **7**, 2936–2943.
180 I. Jeong, C. B. Kim, D. G. Kang, K. U. Jeong, S. G. Jang, N. H. You, S. Ahn, D. S. Lee and M. Goh, *J. Polym. Sci., Part A: Polym. Chem.*, 2019, **57**, 708–715.
181 S. Sæther, M. Falck, Z. Zhang, A. Lervik and J. He, *Macromolecules*, 2021, **54**, 6563–6574.
182 H. Subramanyan, W. Zhang, J. He, K. Kim, X. Li and J. Liu, *J. Appl. Phys.*, 2019, **125**, 095104.
183 Y. Xue, S. Lofland and X. Hu, *Polymers*, 2019, **11**, 456.
184 D. Luo, C. Huang and Z. Huang, *J. Heat Transfer*, 2017, **140**, 031302.
185 Z. Guo, D. Lee, Y. Liu, F. Sun, A. Sliwinski, H. Gao, P. C. Burns, L. Huang and T. Luo, *Phys. Chem. Chem. Phys.*, 2014, **16**, 7764–7771.
186 T. Luo, K. Esfarjani, J. Shiomi, A. Henry and G. Chen, *J. Appl. Phys.*, 2011, **109**, 074321.
187 J. He and J. Liu, *J. Appl. Phys.*, 2021, **130**, 225101.
188 Y. Zhao, X. Zeng, L. Ren, X. Xia, X. Zeng and J. Zhou, *Mater. Chem. Front.*, 2021, **5**, 5617–5638.
189 A. B. Robbins, S. X. Drakopoulos, I. Martin-Fabiani, S. Ronca and A. J. Minnich, *Proc. Natl. Acad. Sci. U. S. A.*, 2019, **116**, 17163–17168.
190 S. E. Regan and D. Greig, *Phys. B: Condens. Matter*, 1990, **165–166**, 909–910.
191 G. Kikugawa, T. G. Desai, P. Keblinski and T. Ohara, *J. Appl. Phys.*, 2013, **114**, 034302.
192 A. B. Robbins and A. J. Minnich, *Appl. Phys. Lett.*, 2015, **107**, 201908.
193 P. M. Smith, L. Su, W. Gong, N. Nakamura, B. Reeja-Jayan and S. Shen, *RSC Adv.*, 2018, **8**, 19348–19352.
194 A. Weathers, Z. U. Khan, R. Brooke, D. Evans, M. T. Pettes, J. W. Andreasen, X. Crispin and L. Shi, *Adv. Mater.*, 2015, **27**, 2101–2106.
195 S. Yu, C. Park, S. M. Hong and C. M. Koo, *Thermochim. Acta*, 2014, **583**, 67–71.
196 L. Sun, G. Yuan, L. Gao, J. Yang, M. Chhowalla, M. H. Gharahcheshmeh, K. K. Gleason, Y. S. Choi, B. H. Hong and Z. Liu, *Nat. Rev. Dis. Primers*, 2021, **1**, 5.
197 M. E. Alf, A. Asatekin, M. C. Barr, S. H. Baxamusa, H. Chelawat, G. Ozaydin-Ince, C. D. Petruczok, R. Sreenivasan, W. E. Tenhaeff, N. J. Trujillo, S. Vaddiraju, J. Xu and K. K. Gleason, *Adv. Mater.*, 2010, **22**, 1993–2027.
198 D. Bilger, S. Z. Homayounfar and T. L. Andrew, *J. Mater. Chem. C*, 2019, **7**, 7159–7174.
199 A. Asatekin, M. C. Barr, S. H. Baxamusa, K. K. S. Lau, W. Tenhaeff, J. Xu and K. K. Gleason, *Mater. Today*, 2010, **13**, 26–33.
200 A. J. Schmidt, X. Chen and G. Chen, *Rev. Sci. Instrum.*, 2008, **79**, 114902.
201 J. C. Duda, P. E. Hopkins, Y. Shen and M. C. Gupta, *Appl. Phys. Lett.*, 2013, **102**, 251912.
202 S. Chen, T. Luan, C. Di, M. H. Lu, X. J. Yan, C. Song and T. Deng, *RSC Adv.*, 2022, **12**, 1897–1903.
203 J. Heinze, B. A. Frontana-Uribe and S. Ludwigs, *Chem. Rev.*, 2010, **110**, 4724–4771.
204 C. R. Martin, *Acc. Chem. Res.*, 1995, **28**, 61–68.
205 W. Lee and S. J. Park, *Chem. Rev.*, 2014, **114**, 7487–7556.
206 L. Shi, D. Li, C. Yu, W. Jang, D. Kim, Z. Yao, P. Kim and A. Majumdar, *J. Heat Transfer*, 2003, **125**, 881–888.
207 M. T. Pettes and L. Shi, *Adv. Funct. Mater.*, 2009, **19**, 3918–3925.
208 A. Weathers, K. Bi, M. T. Pettes and L. Shi, *Rev. Sci. Instrum.*, 2013, **84**, 084903.
209 W. Sha, H. Wang and F. Guo, *J. Mater. Sci.*, 2022, **57**, 5346–5357.
210 J. O. Zoppe, N. C. Ataman, P. Mocny, J. Wang, J. Moraes and H.-A. Klok, *Chem. Rev.*, 2017, **117**, 1105–1318.
211 A. Olivier, F. Meyer, J. M. Raquez, P. Damman and P. Dubois, *Prog. Polym. Sci.*, 2012, **37**, 157–181.
212 X. Yang, X. Zhong, J. Zhang and J. Gu, *Mater. Sci. Technol.*, 2021, **68**, 209–215.
213 K. Ruan, X. Zhong, X. Shi, J. Dang and J. Gu, *Mater. Today Phys.*, 2021, **20**, 100456.
214 Q. Zhang, G. Chen, K. Wu, J. Shi, L. Liang and M. Lu, *J. Appl. Polym. Sci.*, 2020, **137**, 49143.
215 T. Steiner, *Angew. Chem., Int. Ed.*, 2002, **41**, 48–76.
216 N. Mehra, M. Jeske, X. Yang, J. Gu, M. A. Kashfipour, Y. Li, J. A. Baughman and J. Zhu, *ACS Appl. Polym. Mater.*, 2019, **1**, 1291–1300.
217 L. Mu, J. He, Y. Li, T. Ji, N. Mehra, Y. Shi and J. Zhu, *J. Phys. Chem. C*, 2017, **121**, 14204–14212.
218 R. J. Roe, *Methods of X-ray and Neutron Scattering in Polymer Science*, Oxford University Press, 2000.
219 C. Andreani, D. Colognesi, J. Mayers, G. Reiter and R. Senesi, *Adv. Phys.*, 2005, **54**, 377–469.
220 B. S. Hudson, *J. Phys. Chem. A*, 2001, **105**, 3949–3960.
221 A. A. Shcherbakov, J. Medeiros-Silva, N. Tran, M. D. Gelenter and M. Hong, *Chem. Rev.*, 2022, **122**, 9848–9879.

Published on 14 June 2022. Downloaded on 2/13/2026 4:19:27 PM.

222 S. P. Danielsen, H. K. Beech, S. Wang, B. M. El-Zaatari, X. Wang, L. Sapir, T. Ouchi, Z. Wang, P. N. Johnson and Y. Hu, *Chem. Rev.*, 2021, **121**, 5042–5092.
223 M. R. Hansen, R. Graf and H. W. Spiess, *Chem. Rev.*, 2016, **116**, 1272–1308.
224 J. Koenig, *Appl. Spectrosc. Rev.*, 1971, **4**, 233–305.
225 A. Kuptsov and G. N. Zhizhin, *Handbook of Fourier Transform Raman and Infrared Spectra of Polymers*, Elsevier, 1998.
226 V. Bershtein and V. Ryzhov, in *Polymer Analysis and Characterization*, Springer, 1994, pp. 43–121.
227 D. Zhao, X. Qian, X. Gu, S. A. Jajja and R. Yang, *J. Electron. Packag.*, 2016, **138**, 040802.
228 B. Abad, D. A. Borca-Tasciuc and M. Martin-Gonzalez, *Renewable Sustainable Energy Rev.*, 2017, **76**, 1348–1370.
229 D. Kraemer and G. Chen, *Rev. Sci. Instrum.*, 2014, **85**, 025108.
230 H. Natesan and J. C. Bischof, *ACS Biomater. Sci. Eng.*, 2017, **3**, 2669–2691.
231 D. H. Olson, J. L. Braun and P. E. Hopkins, *J. Appl. Phys.*, 2019, **126**, 150901.
232 R. J. Pylkki, P. J. M. P. J. Moyer and P. E. W. P. E. West, *Jpn. J. Appl. Phys.*, 1994, **33**, 3785–3790.
233 W. Parker, R. Jenkins, C. Butler and G. Abbott, *J. Appl. Phys.*, 1961, **32**, 1679–1684.
234 D. G. Cahill, *MRS Bull.*, 2018, **43**, 782–789.
235 X. Qian, Z. Ding, J. Shin, A. J. Schmidt and G. Chen, *Rev. Sci. Instrum.*, 2020, **91**, 064903.
236 P. Jiang, X. Qian and R. Yang, *J. Appl. Phys.*, 2018, **124**, 161103.
237 C. Dames, *Annu. Rev. Heat Transfer*, 2013, **16**, 7–49.
238 W. N. dos Santos, P. Mummery and A. Wallwork, *Polym. Test.*, 2005, **24**, 628–634.
239 C. Choy, W. Leung and Y. Ng, *J. Polym. Sci., Part B: Polym. Phys.*, 1987, **25**, 1779–1799.
240 H. Mehling, G. Hautzinger, O. Nilsson, J. Fricke, R. Hofmann and O. Hahn, *Int. J. Thermophys.*, 1998, **19**, 941–949.
241 R. Rudkin, R. Jenkins and W. Parker, *Rev. Sci. Instrum.*, 1962, **33**, 21–24.
242 H. Ohta, H. Shibata and Y. Waseda, *Rev. Sci. Instrum.*, 1989, **60**, 317–321.
243 H. Shibata, H. Ohta and Y. Waseda, *Mater. Trans., JIM*, 1991, **32**, 837–844.
244 Y. Tada, M. Harada, M. Tanigaki and W. Eguchi, *Rev. Sci. Instrum.*, 1978, **49**, 1305–1314.
245 R. Coquard and B. Panel, *Int. J. Therm. Sci.*, 2009, **48**, 747–760.
246 Y. Kogure, T. Mugishima and Y. Hiki, *J. Phys. Soc. Jpn.*, 1986, **55**, 3469–3478.
247 C. A. Paddock and G. L. Eesley, *J. Appl. Phys.*, 1986, **60**, 285–290.
248 W. Capinski, H. Maris, T. Ruf, M. Cardona, K. Ploog and D. Katzer, *Phys. Rev. B: Condens. Matter Mater. Phys.*, 1999, **59**, 8105.
249 X. Wang, C. D. Liman, N. D. Treat, M. L. Chabinyc and D. G. Cahill, *Phys. Rev. B: Condens. Matter Mater. Phys.*, 2013, **88**, 075310.
250 J. P. Feser and D. G. Cahill, *Rev. Sci. Instrum.*, 2012, **83**, 104901.
251 J. Zhu, H. Park, J. Y. Chen, X. Gu, H. Zhang, S. Karthikeyan, N. Wendel, S. A. Campbell, M. Dawber and X. Du, *Adv. Electron. Mater.*, 2016, **2**, 1600040.
252 D. G. Cahill, *Rev. Sci. Instrum.*, 2004, **75**, 5119–5122.
253 A. Schmidt, M. Chiesa, X. Chen and G. Chen, *Rev. Sci. Instrum.*, 2008, **79**, 064902.
254 M. Nonnenmacher and H. Wickramasinghe, *Appl. Phys. Lett.*, 1992, **61**, 168–170.
255 S. Gomès, P. Newby, B. Canut, K. Termentzidis, O. Marty, L. Frechette, P. Chantrenne, V. Aimez, J. M. Bluet and V. Lysenko, *Microelectron. J.*, 2013, **44**, 1029–1034.
256 D. I. Florescu, L. Mourokh, F. H. Pollak, D. C. Look, G. Cantwell and X. Li, *J. Appl. Phys.*, 2002, **91**, 890–892.
257 M. J. Assael, C. F. Chen, I. Metaxa and W. A. Wakeham, *Int. J. Thermophys.*, 2004, **25**, 971–985.
258 Y. Gu, X. Ruan, L. Han, D. Zhu and X. Sun, *Int. J. Thermophys.*, 2002, **23**, 1115–1124.
259 A. Majumdar, J. Carrejo and J. Lai, *Appl. Phys. Lett.*, 1993, **62**, 2501–2503.
260 C. Williams and H. Wickramasinghe, in *Photoacoustic and Photothermal Phenomena*, Springer, 1988, pp. 364–369.
261 K. Kim, W. Jeong, W. Lee and P. Reddy, *ACS Nano*, 2012, **6**, 4248–4257.
262 W. Lee, K. Kim, W. Jeong, L. A. Zotti, F. Pauly, J. C. Cuevas and P. Reddy, *Nature*, 2013, **498**, 209–212.
263 K. Luo, Z. Shi, J. Lai and A. Majumdar, *Appl. Phys. Lett.*, 1996, **68**, 325–327.
264 A. Majumdar, *Annu. Rev. Mater. Sci.*, 1999, **29**, 505–585.
265 J. Barnes, R. Stephenson, M. Welland, C. Gerber and J. Gimzewski, *Nature*, 1994, **372**, 79–81.
266 A. Pope, B. Zawilski and T. Tritt, *Cryogenics*, 2001, **41**, 725–731.
267 N. J. Hines, L. Yates, B. M. Foley, Z. Cheng, T. L. Bougher, M. S. Goorsky, K. D. Hobart, T. I. Feygelson, M. J. Tadjer and S. Graham, *Rev. Sci. Instrum.*, 2021, **92**, 044907.
268 T. Borca-Tasciuc and G. Chen, in *Thermal Conductivity*, Springer, 2004, pp. 205–237.
269 B. M. Zawilski, R. T. Littleton IV and T. M. Tritt, *Rev. Sci. Instrum.*, 2001, **72**, 1770–1774.
270 D. R. Flynn, in *Compendium of Thermophysical Property Measurement Methods*, Springer, 1992, pp. 33–75.
271 O. Maldonado, *Cryogenics*, 1992, **32**, 908–912.
272 J. Lee, Z. Li, J. P. Reifenberg, S. Lee, R. Sinclair, M. Asheghi and K. E. Goodson, *J. Appl. Phys.*, 2011, **109**, 084902.
273 J. A. Malen, K. Baheti, T. Tong, Y. Zhao, J. A. Hudgings and A. Majumdar, *J. Heat Transfer*, 2011, **133**, 081601.
274 D. Rodin and S. K. Yee, *Rev. Sci. Instrum.*, 2017, **88**, 014902.

 This journal is © The Royal Society of Chemistry 2022

275 J. Yang, E. Ziade, C. Maragliano, R. Crowder, X. Wang, M. Stefancich, M. Chiesa, A. K. Swan and A. J. Schmidt, *J. Appl. Phys.*, 2014, **116**, 023515.
276 J. Zhu, D. Tang, W. Wang, J. Liu, K. W. Holub and R. Yang, *J. Appl. Phys.*, 2010, **108**, 094315.
277 P. Jiang, X. Qian and R. Yang, *Rev. Sci. Instrum.*, 2018, **89**, 094902.
278 M. Li, J. S. Kang and Y. Hu, *Rev. Sci. Instrum.*, 2018, **89**, 084901.
279 A. Z. Zhao, M. C. Wingert and J. E. Garay, *J. Chem. Eng. Data*, 2020, **66**, 262–270.

Published on 14 June 2022. Downloaded on 2/13/2026 4:19:27 PM.